Ministry of Higher Education and Scientific Research
University of Baghdad
Institute of Laser for Postgraduate Studies

Sub Surface Engraving of BK7 and PMMA using Q-Switched Nd:YAG Laser

A Thesis Submitted to the Institute of Laser for Postgraduate Studies, University of Baghdad in Partial Fulfillment of the Requirements for the Degree of Master of Science in Laser / Mechanical Engineering

By
Zahraa Mohammed Saleh

B.Sc. Mechanical Engineering 2006

Supervisor
Dr.Ziad Aeyad Taha

2017 AD   **1438 AH**

Acknowledgment

I would like to express my deep gratitude to my supervisor, Dr.Ziad Aeyad Taha, Head of engineering and Industrial Application department . I have learned many things since I became his student. He taught me how to search literature and how to collect data.

I am also grateful to Prof. Dr.Abdul Hadi M.Al-Janabi , Dean of Institute of Laser for Postgraduate Studies/University of Baghdad for his kind support overcome hardships.

Also I would like to thank Ass.Prof.Dr.Mahammed K.Dhahir, Assistant Dean of Institute of Laser for Postgraduate Studies in University of Baghdad for his assistance .

In addition, I want to acknowledge Prof. Mazin M. Elias, Asst Prof. Hussain Ali Jawad, Dr.Thaier Abid Tawfiq ,and Ass.Prof Dr. Shelan Khasro Twfeeq. I appreciate every minute they have been spent to guide me in my research.

Deep gratitude goes to Dr. Mahmoud Shakir Mahmoud, for his support during the courses and the research.

I would like to thank Dr. Fadil Abass,and Dr.Ahmed Mohammed Hasan for their kind help and support.

Also I would like to thank Dr. Abdul Kareem Mohammed Ali Al-Sameraiy / department of chemistry / College of Science in Baghdad University.

Special thanks go to Eng. Atheer Rasheed , Eng. Ahmed Abdul Rezaq and Eng. Vian Jabar Jumaa for their kind support and help.

Special thanks are given to my dearest friends Farah ,Shaimaa,Heba Sura and Marwa and all the staff of Institute of Laser for Postgraduate Studies. where most of my Practical experience has been built.

Last but not least , I owe more than thanks to my family members: my parents, husband, my   brother and my sisters for their support and encouragement throughout my life. Without their support, it was impossible for me to finish my college and graduate education .

Zahraa Mohammed Saleh

Abstract

Sub surface Laser Engraving is a technique used for marking transparent materials. It can be carried out by focusing pulsed laser beam inside the transparent material.

In this study sub surface laser engraving application was achieved using Q-switched Nd:YAG laser, Two systems for Nd:YAG laser with different parameters were used. The first was 1064 nm wave length , 4ns pulse duration and the second was 1064nm and 532nm wavelengths having 10ns pulse duration.

Two different transparent materials were used in this work which are borosilicate crown glass (BK7) and poly methyl methacrylate (PMMA) with thickness 10 mm for both materials.

Effect of changing laser energy ,wavelength ,focal position ,number of pulses, feed rate (CNC speed) and pulse repetition rate were studied to determine the best dot by using transmission microscope and scanning electron microscope. Dots morphology, shapes, area and resolution were realized .Dots area and penetration depth were determined . The dots area increased as the laser energy increased, The resolution of the image can be controlled by changing CNC feed rate and pulse repetition rate .The best results was achieved with green light of 532nm,The following parameters were applied to do the job : feed rates of 2.5mm/s and 4.3mm/s , energy of 360 mJ at 6Hz pulse repetition rate and 460 mJ energy at 5Hz pulse repetition rate and the minimum was at feed rate1.56 mm/s and 8.5mm/s energy 360 mJ pulse duration 6Hz..

Sub surface laser engraving has been simulated by using COMSOL Multiphysics. The heat transfer model provide temperature distribution inside the material and dots dimensions have been measured and compared with the experimental results ,and they almost showed a reasonable matching with experimental results.

List of Contents

Chapter One Introduction Basic Concepts

Chapter Two Meterials and Methodes

List of Figures

List of Tables

List of Abbreviations

2D	Two dimensions
3D	Three dimensions
ArF	Argon Fluoride
BK7	Borosilicate crown glass
CCD	Charge –Coupled Device
CNC	Computerized numerical control
CO_2	Carbon dioxide
CW	Continuous wave
EDX	Energy dispersive X-ray spectroscopy
f.p.p	Focal plane position
KrF	Krypton Fluoride
KTP	Potassium titanyl phosphate
Nd-YAG	Neodymium-yttrium aluminum garnet
P.R.R	Pulse repetition rate
PMMA	Poly methyl methacrylate
SEM	Scanning electron microscope
SSLE	Sub surface laser engraving
Ti	Titanium
UV	Ultra violet
VIS	Visible

List of Symbols

symbol	Description	Units
A	cross-sectional area	m^2
a	laser beam reduce	μm
dT/dx	temperature gradient	$K \cdot m^{-1}$
E	energy	J
I	Power density	W/cm^2
K	Thermal conductivity	$W \cdot m^{-1} \cdot K^{-1}$
P	The incident laser power	(W)
Q	Heat generation rate	W/cm^2
q	heat transfer by conduction	W
R	Reflectivity	-
r	Redial thermal distribution	μm
z	Thermal depth of penetration	μm
α	Absorption coefficient	cm^{-1}
λ	Wavelength	m
τ	Pulse duration	sec.

Introduction
and
Basic Concepts

1.1 Introduction

Laser marking /engraving is a non-contact process which means producing permanent images with high resolution on most of engineering materials. The most popular laser sources for marking are CO_2 laser, Nd:YAG laser, fiber laser and excimer laser with levels of several tens of watts average power [1][2].

Laser marking /engraving differs from other traditional marking techniques that either use ink or bit heads. Laser marking is widely used in large number of applications such as adding parts numbers, expiry dates on food packages manufacturing, medicines, adding traceable information for quality control, printing bar codes, logos and other products information [3].

Surface marking of glass is done with either excimer lasers or CO_2-laser. These lasers have power that is high enough to induce an ablation process on relatively large areas. For this technology, lasers with good beam quality and high pulse repetition rate like solid state CW -pumped lasers are required. Unfortunately glass is highly transparent for 1.06 μm wavelength commonly used. Using absorption via non-linear effects can be a solution for this problem [4][5] .

One of the unique applications that lasers offer is to modify the bulk of transparent materials, without surface damage which is sometimes called subsurface laser engraving (SSLE). Applications of subsurface processing are the fabrication of complex three-dimensional objects, the production of optical components, and data storage [6].

Subsurface laser engraving is performed by a computer-controlled device where a laser beam is focused inside the material to produce a tiny spot (dots) inside transparent materials bulk, locally destroying the transparency of this

material due to refractive index change   or increases in thermal absorption caused by laser energy inside the material, also these dotes may results from micro explosion occur inside the material [7][8].

These dots are gathered to form the image through a matrix. Many parameters like pulse energy, pulse duration, pulse repetition rate and the laser wavelength affect the dot size as well as repeating more than one pulse in the same place [9].

1.2 Laser material interaction

Laser material interaction processes are divided into four major classes, heating (without melting/vaporizing), melting (no vaporizing), vaporizing and plasma formation, all these processes are a function of laser power and interaction time [11].

1.2.1 Heating

When a laser beam hits the surface of material, it results in excitation of free electrons (in metals), vibrations (in insulators), or both (in semiconductors). This excitation energy is converted into a heat without any phase transformation. Subsequently it is followed by diverse heat transfer processes such as conduction into the materials, convection and radiation from the surface. The most significant heat transfer process is the heat conduction into the material [12]. Laser heating below melting threshold can activate a variety of temperature dependent processes within the solid material .The flow of heat is described by Fourier's laws on heat conduction – a flux equation[13]

q= -kA(dT/dx)   ….(1.1)

Where,

'q' heat transfer by conduction (W)

'k' is the thermal conductivity of the material $(W \cdot m^{-1} \cdot K^{-1})$

'A' is the cross-sectional area normal to the direction of heat flow (m^2) and

'dT/dx' is the temperature gradient $(K \cdot m^{-1})$

1.2. 2. Melting

If the material absorb a sufficient energy from the laser, then the molecular vibration becomes so intense that the molecular bonding is stretched so far,

that it is no longer capable of exhibiting mechanical strength and the material is said to be melted. When the surface temperatures of the material override the point of melting, it cause transformation in the material phase due to continuity of laser irradiation [14].

1.2.3. Vaporization

On further heating, the bonding is further loosened due to the strong molecular vibrations and the material is said to be evaporated. It happens once the temperature reaches the boiling threshold, that is why it needs high laser irradiance (more than 10^6 W/cm^2) when melting become less significant and vaporization takes place [2][14].

1.2.4. Plasma formation

Once the vaporization is initiated, the interactions between the resulting vapor and the incident laser beam become important. One of the most important interactions is the ionization of vapor. The highly ionized vapor is termed as plasma which is occurred when laser irradiation is more than 10^9 W/cm^2 .The plasma continues as long as the laser does [14][12].

The sequence of absorption stages is illustrated in Figure (1.1).
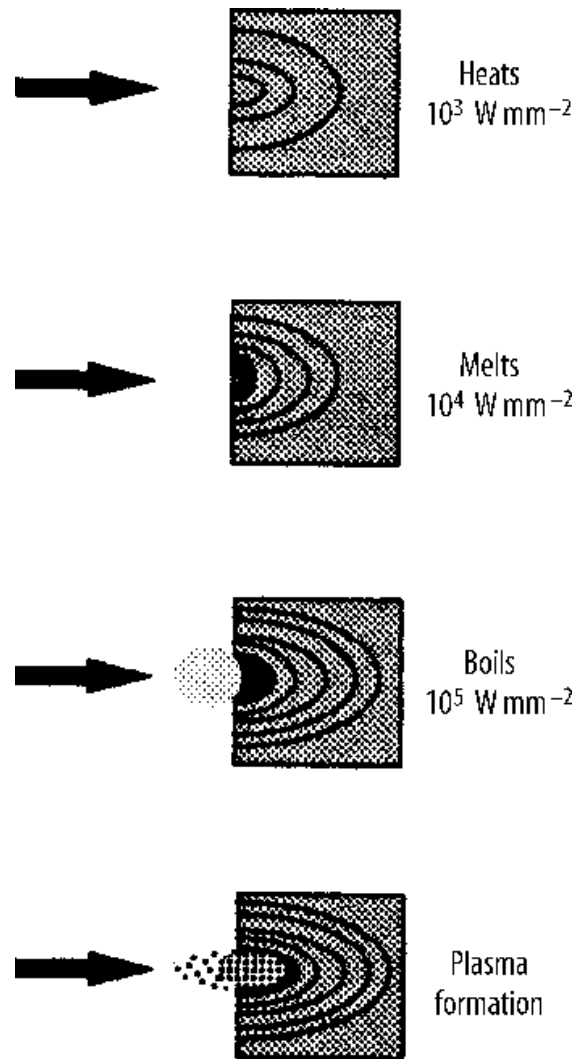
Figure 1.1 Sequence of absorption events varying with absorbed power [14]

1.3 Laser material processing

In general, applications of laser in material processing can be grouped into two major classes [10]:

(a) Applications requiring limited energy/power and causing no significant change in phase or state.

(b) Applications requiring substantial amount of energy to induce the phase transformations.

The first type includes semiconductor annealing and etching, polymer curing, marking of integrated circuit substrates. The second type of application encompasses cutting, welding, fusion and heat treatments. The average power and efficiency of lasers are not of that important for the former category which involves no change in phase [10,11].

Lasers suitable for this group of applications include (but not limited to) excimer lasers (KrF, ArF), ion lasers, metallic vapor lasers (cadmium, selenium, copper, gold), solid state lasers (Nd:YAG, Nd:glass), semiconductor lasers (gallium aluminum arsenide,etc.), and molecular lasers (CO_2, CO, etc.). For the second category, laser power efficiency and interaction-time are crucial as the processes involve single or multiple phase changes within a very short time. Because of high-energy requirement, for this class of operations, CO_2 and Nd:YAG lasers are practically the only choices[10,11].

In the domain of laser marking and engraving, fiber lasers have almost completely displaced diode-pumped and flash-lamp-pumped solid-state lasers. The only exception is Co_2lasers are used in non-metal engraving [15].

Figure (1.2) shows various laser–material interactions and their applications in materials processing.
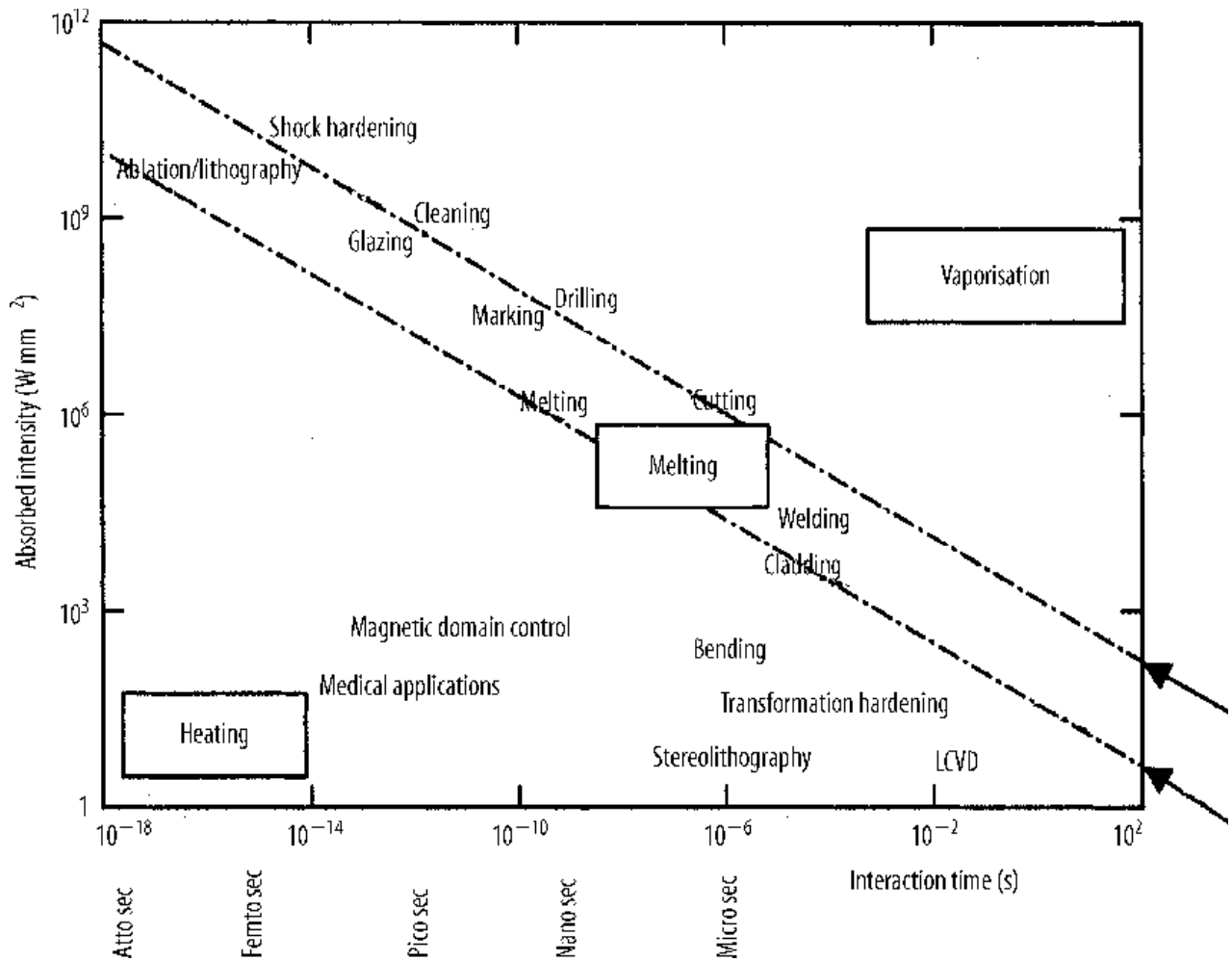
Figure1. 2 Laser processes mapped against power density and interaction time [14]

1.4 Laser marking and engraving

Laser marking is a rapid, non-contact means of producing permanent high resolution images on the surface of most engineering materials. The beam may be scanned over the material using computer-controlled mirrors oscillating along orthogonal axes, or projected through a mask or stencil to generate the image [2].

The impact of laser engraving has been more pronounced for specially-designed "laserable" materials. These include laser-sensitive polymers and

novel metal alloys. The point where the laser beam touches the surface should be on the focal plane of the optical system of laser, and is usually identical with its focal point. This point is typically small, perhaps less than a fraction of a millimeter (depending on the optical wavelength). Only the area inside this focal point is significantly affected by the laser beam, whether the focal point was on the surface or inside the material. The energy delivered by the laser change the material in the focal point [10].

The laser marking mechanisms can be divided in two major classes:

- Material removal/addition
- Material modification, as illustrated in Figure 1.3
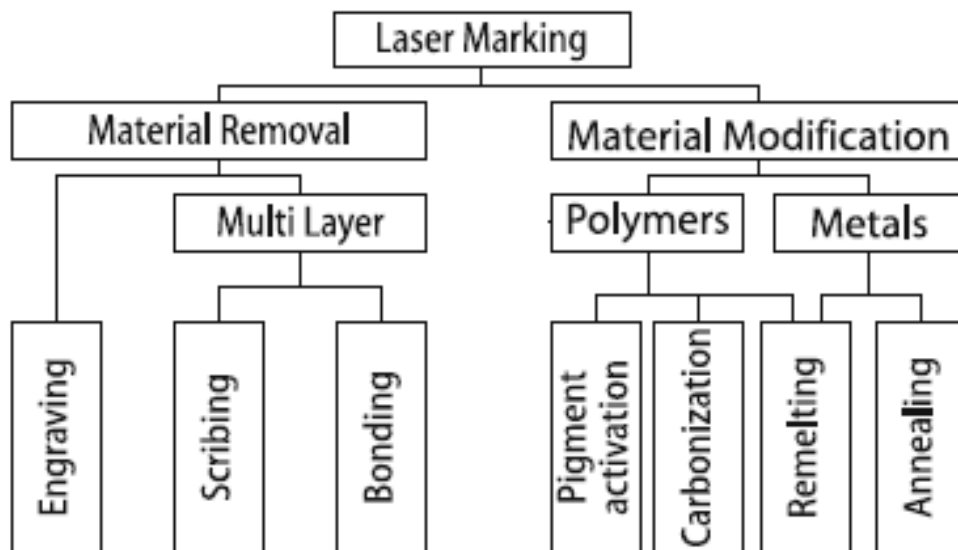
Figure 1.3 General classification of laser marking [4]

1.4.1 Laser marking by material removal or addition

The first type of laser marking using material removal is engraving which may produce burr or redeposits that require cleaning processes for the redeposits. Engraving is able to produce good resolution but thermal impact might be happened.

Besides engraving, there are two other techniques used, bonding and scribing. These require coating of the surface of the material.

In bonding process the laser is used to heat and melt the layer and the workpiece intended to be marked. Scribing process, is removing the coating layer while only the area heated with laser not removed from the workpiece surface [13].

1.4.2 Laser marking by material modification

The second class of laser marking techniques depends on material modification this include four types: annealing, remelting, pigment activation, and carbonization.

Annealing is a marking technique which is often used for metals. It is occurred due to the reaction between material heated by laser and ambient gases that can lead to material colorization, with quite low resolution and contrast, but the surface geometry has no changes.

Remelting can be carried out on both metals and polymers. Remelting of polymers often leads to gas emission due to chemical processes in the bulk polymer. It produces different surface morphologies of the resolidified material that leads to a good visibility. During resolidification the emitted gas is trapped and forms pores, these pores lead to a diffusing reflection and scattering of light. Markings created by polymer remelting can also lead to a modification of chemical properties. The resolution is low compared to carbonization and pigment activation.

Pigment activation is a marking process for specifically prepared polymers. Additives that can be chemically excited by laser radiation are required for this kind of marking. Pigment activation leads to a good contrast and resolution but suffers from the necessity for the additive material. The great advantages of pigment activation is that no melting and vaporization is happened so the thermal impact is very low .The last type of laser marking by material modification is Carbonization which also can be applied on a polymers. It is based on a chemical reaction below the polymer surface induced by laser radiation. There is no change

of the chemical or physical properties of the material surface in Carbonization technique. Therefore, it is widely used in medical applications [2,13].

1.5 Sub surface Laser Engraving

Is the process of engraving an image in a transparent solid material by focusing a laser below the surface to create small damage (which basically consists of dots and surrounding cracks) as shown in Figure (1.4a). Short pulse laser tightly focused inside the bulk of a transparent solid could produce three-dimensional (3D) structures with a controlled size. It has also been demonstrated that these structures can be formed in different spatial arrangements as shown in Figure (1.4b) [17].

(a)   (b)
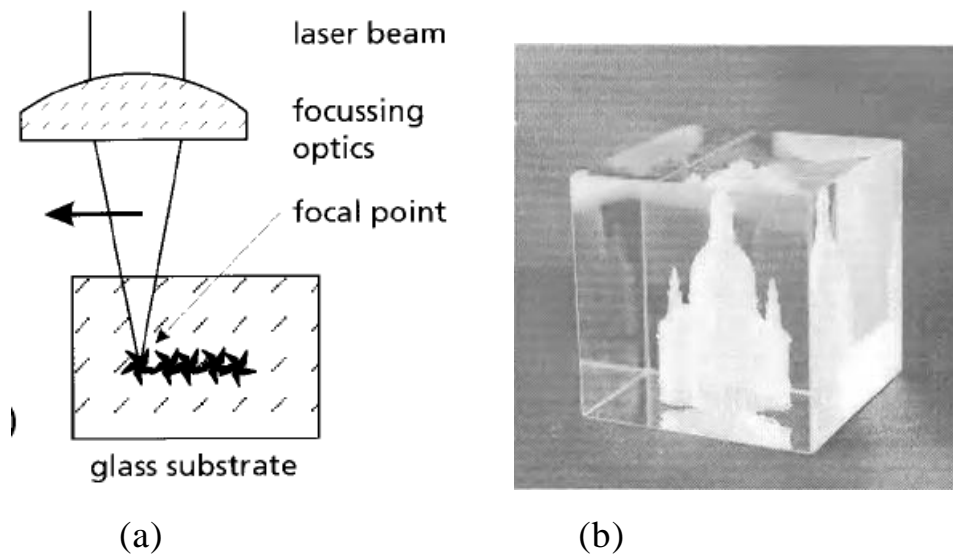
Figure 1.4 Image of internal modification in a transparent material interacted by laser [5,46].

Such engraved materials are of high-grade optical quality (suitable for lenses, with low dispersion) to minimize distortion of the beam. BK7 glass is a common material for this application. Plastics are also used. It is possible to compose 2D- and 3D-objects by programmed relative motion between laser beam and target [5,10].

The two-dimensional or three-dimensional images / portrait image are converted into a points cloud, and the points arrangement is in accordance with the control software to control laser position and the laser crystal output. When the crystal is in a particular location, a focused laser will hit a little bursting point in the crystal interior, as well as a large number of small bursting points in the formation of an image to be engraved / Portrait [19].

1.6 Mechanisms of Sub-surface Laser Engraving

Absorption of a laser beam that is incident on a material occurs by linear or nonlinear processes. The absorption results in heating of material in the focal region first to the melting temperature and then to the vaporization temperature, depending on the beam intensity and pulse duration. For radiation outside the ultraviolet range, the absorption mechanisms are different for absorbent materials such as metals and semiconductors, transparent dielectric materials such as glasses and plastics. If a light beam propagates in a homogeneous medium, the light intensity decrease exponentially along the path according to Lambert's law of absorption [20].

Absorption also depends on laser intensity. For opaque materials, absorption is linear when the beam pulse duration is long (10^{-3}-10^{-6} s) and the intensity is low, while nonlinear absorption becomes dominant when the pulse duration is short (10^{-9} -10^{-15} s) and the intensity is high. Absorption for transparent materials results mainly from nonlinear process [21].

For optical breakdown and material damage to occur, a nonlinear absorption mechanism must deposit laser energy into the material by promoting electrons from the valence band to the conduction band. There are two classes of nonlinear excitation mechanisms that play a role in this absorption, photoionization and

avalanche ionization. If enough laser energy is deposited into the material by these nonlinear absorption mechanisms, permanent damage is produced [22]. The absorption can be increased for shorter wavelengths where the photon energy becomes larger than the band-gap value or if the incident light intensity increases to the level where the multi-photon processes become important [17]. There is a fundamental dependence of the laser–matter interaction on the focusing conditions; either the laser beam is focused on the surface or laser beam is tightly focused inside a transparent material. In the former case the interaction zone containing high energy density is confined inside a cold and dense solid material. For this reason, the hydrodynamic expansion is insignificant if the energy density is lower than the structural damage threshold, but above this threshold it is highly affective. This results in a change in the optical and structural properties in the affected region. There are two different ways for inducing the changes in a bulk solid material by laser effect. First, non-destructive phase that can be induced by laser at the intensity below the damage threshold. Second, irreversible structural changes may be produced at high intensity above the optical breakdown threshold [17][18].

When a laser pulse with energy above the damage threshold is focused into a bulk of glass, it leads to a micro explosion. The multi-photon absorption and avalanche ionization creates high density electron plasma, and the transfer of energy from the electron plasma to the lattice leads to high temperature and high pressure, which forces the material from the center outwards. This leads to the formation of a damaged structure. When the energy of the laser pulse is lower than the damage threshold, the plasma density is not high enough to induce damage, but it could induce color centers and lattice defects, and high temperature and pressure could induce local stress and densification, which contribute to the increase of refractive index [23].

There are generally two main mechanisms which cause damage. The first one is thermal absorption, which arises from deposition of the laser energy in the material. This process may be generally observed during radiation of continuous wave, long pulse lengths, and high pulse-repetition-frequency pulse trains. The second one is electron avalanche, which arises when the electric field density is high enough or the energy is delivered at a high intensity to strip electrons from the lattice. These applied when the pulse lengths are short enough for avalanche ionization to take place and when the thermal absorption is low enough for the avalanche threshold to be below the thermal threshold. Damage may be caused by single mechanism or both of the above mechanisms .Table (1.1) clarifies the relationships between the pulse length of high-power laser and the mechanisms that cause damage [24].

Table (1.1) The relationships between the pulse length and damage mechanisms [24]

Laser pulse length	Damage mechanisms	Damage phenomena
Long pulse Continuous wave	Thermal absorption	Stress, strain, melting, and ablation
Short pulse for ns level	Impact ionization	Micropits, debris
Extremely short pulse for ps level	Impact ionization	Crater, plasma, and crush
Ultrashort pulse for fs level	Multiphoton-assisted impact ionization	Crater, plasma, crush, and cracks

The most effective damage mechanism, is the thermal explosion due to nonlinear heating and thermal UV-photoionization of the surrounding material and the impact ionization, which dominated at long laser pulse durations (mostly in nanosecond duration range)[25].

The modified area inside the material (dots) is depends on many experimental parameters: E (the pulse energy) which should be high enough to produce a damage (dot)inside the material, τ (the pulse duration) if it is long the dots shape will be irregular and cracks appear in the material even at energies only slightly above the material damage threshold ,also the wave length effect the damage e size and morphology. Damage mechanisms are differs at longer wavelengths from short wave length damage. Two-photon absorption occurs through short wavelength (266nm), whereas at longer wavelengths the two-photon process does not occur ,However, under special conditions, exposure to multiple pulses in the same place can change the damage size [9,26,27].

1.7 Sources for subsurface laser engraving

1.7.1 Nd-YAG laser

Neodymium-doped yttrium aluminum garnet is the most important and most widely used solid-state laser because of its good thermal and mechanical properties. The more popular SSLE engraving machines use the Diode Pumped Solid State laser. In the past few years, the use of SSLE has become more cost effective to produce 3D images in souvenir 'crystal' or promotional items [10].

Main wavelength 1064 nm, second harmonic 532 nm and third harmonic λ=355 nm are all suitable for this kind of application [28].

1.7.2 Titanium - Sapphire or Femtosecond Laser

Generation of femtosecond laser pulses requires a medium with a broadband gain spectrum together with an active or passive mode-locking mechanism. Femtosecond lasers have opened up new avenues in materials processing due to their unique characteristics of ultrashort pulse widths and extremely high peak intensities. One of the most important features of femtosecond laser processing is that a femtosecond laser beam is highly absorbable in even

transparent materials due to nonlinear multiphoton absorption. Multiphoton absorption enables both surface and internal three-dimensional modification and microfabrication of transparent materials such as glasses. This make it is possible to directly fabricate three-dimensional microfluidic, microelectronic, and micro-optical components in the glass[29,30].

1 .8 Borosilicate crown glass Bk7

Glass is an amorphous material, which is often, but not always, derived from a molten liquid. Classifications of glass according to chemical composition include 3 main groups: soda-lime glass, lead glass and borosilicate glass. Glass can be marked in different ways; one of them is glass optical breakdown which is well-known because all 3D images in glass are made with this process. Glass easily form cracks, formation of cracks reduce the high stress caused by the absorption of laser energy. This absorption is limited to the far infrared and UV region of the spectrum. [28,31,32,33]

Borosilicate crown glass has special properties including high optical quality glass, practically free of bubbles and inclusions, very clear and with colorless appearance. BK7 glass is widely used as a low cost technical optical glass for applications in the visible region. The chemical composition of BK7 as specified by Schott includes the following: silica, boron oxide, sodium oxide, potassium oxide, barium oxide, titanium oxide, calcium oxide and impurities in small quantities. This leads to some peculiarities in the electronic structures, lower softening temperature and, notably, a high expansion coefficient (approximately 10 times higher than for fused silica). BK7 has several applications such as general optics ,wave guide writing ,substrates for mirror coatings ,wafers for micro-optics and blanks for lenses [33,34,35].

1.9 Poly Methyl Methacrylate (PMMA)

Polymer is a substance that is composed of molecules which have long sequences of one or more species of atoms or groups of atoms linked to each other by a primary, usually covalent bonds [36]. Polymers are very large molecules, or macromolecules, formed by the union of many smaller molecules. These smaller units are termed monomers before they are converted to polymers [37].

PMMA it is the most important member of the family of acrylic resins, due to its optical clarity (92% light transmission). PMMA molding powders can be injection molded, and compression molded. The PMMA liquid can be cast into rods, sheets, optical lenses, etc. Cast and extruded PMMA sheets are fabricated and thermoformed into many products such as aircraft canopies, skylights, lighting fixtures, and outdoor signs due to their good mechanical strength, acceptable chemical resistance, [38,39].

1.10 Advantages of laser marking and engraving

Laser marking has more advantages than the traditional marking such as [3,5,14]:

1. Conventional marking/engraving employs toxic chemicals, leaving behind a chemical residue.

2. Laser marking /engraving is a non-contact and a quiet process and there is no requirement for any special environment.

3. Since the laser marking machine has no direct contact with the surface of the material to be marked or engraved, it is easier to adapt to uneven surfaces.

4. In conventional engraving, tool tips need to be replaced depending upon the type of surface to be marked or engraved.

5. Laser marking/engraving produces high-quality permanent marks with good readability and good text permanence.

6. Laser marking /engraving is effective even on difficult-to-access areas and adapts very well to automation.

7. Due to precise beam positioning and localized energy transfer, the heat-affected zone is very small this practically eliminates any damage to adjacent areas.

8. Laser marking/engraving is characterized by high reproducibility, high speed and high throughput.

9. Laser marking /engraving can be used effectively on a wide variety of metallic and non-metallic materials of various sizes, shapes and orientations.

1.11 Limitations of laser marking and engraving

In spite of all the advantages of laser marking/ engraving there is still some limitation [5,14,40]

1. High investment costs.

2. Laser marking/engraving machines need skilled operators.

3. Probability of thermal load on workpiece.

4. Laser beam must have special properties like high repetition rate.

5. The treatment is not possible for very thin materials or under internal or external stress: the pulse duration is long enough to produce thermal effects and cracks.

6. Glass containers (engraved bottles of perfumes or juice for instance) must withstand such tough transportation constraints (cold / hot, vibration, shocks) that micro cracks will lead to catastrophic crack growth and possibly bottle collapse.

1.12 Heat transfer equation

The absorption of laser light takes place through photon interaction with bound and free electrons in the material structure, whereby these electrons are raised to higher energies. The further conversion of this energy takes place through various collision processes involving electrons, lattice site phonons, ionized impurities, and defect structures. The mean collision time in this energy transference is of the order of $10^{-12} - 10^{-14}$ s . During the pulses whose pulse duration is 10^{-9} s, the absorbing electrons have time to undergo many collisions. This leads to the equilibrium energy transport in the lattice system, i.e., the laser energy is instantaneously converted to internal energy gain at the point at which absorption takes place [41].

The interaction of the laser with the materials basically causing localized temperature increases. Conventional heat transfer analysis dominates in equilibrium energy transport .When laser hits the material it is assumed that beam penetrate cylinder shape with the direction of laser propagation [41][42] as in Equations(1.1)(1.2) and(1.3)

$Q(r,z)=(\alpha I) \exp(-\alpha z) \exp(-(r/a^2))$ --------(1.2)

Q: the volumetric heat generation inside the material(W/m^3)

I : intensity of laser(W/m^2),can be calculated from Equation (1.3)

$I=(1-R_c)*(P/\pi*a^2)$………..(1.3)

P : is the incident laser power (W)

α :absorption coefficient (1/m)

R_c ;   reflectivity

a: laser beam reduce (m)

r: radial thermal distribution (m)

z: thermal depth of penetration (m)

by solving Equation (1.3)by (1.2) the final heat generation equation is (1.4)

$$Q(r,z) = (1-R_c)*(P/\pi*a^2)* \alpha*\exp(\alpha*-z)*\exp((r/a)^2)\ldots.(1.4)[42][43]$$

1.13 Literature survey

The use of sub-surface laser engraving began before 1990, but it was uncommon at that time. Many studies have been done in this field in order to know more information about this application.

Stuart et al. (1995) investigated that the damage threshold continues to decrease with decreasing pulse width and reported measurements of damage thresholds for fused silica and calcium fluoride at 1053 and 526 nm for pulse durations ranging from 1 ns to 270 fs The damage location is limited to only a small region where the laser intensity is sufficient to produce a plasma with essentially no collateral damage [44].

Glezer et al. (1996) presented novel method for creating 3-D optical data storage by using ultrashort laser pulses (femtosecond laser) method which can also be used for engraving fine scale patterns inside transparent materials without damaging or altering the surface. They found out that the result structures from longer pulses are irregularly shaped, and cracks appear in the material even at energies barely above the damage threshold [27].

N. Kuzuu et al.(1999) suggested that for short wavelength damage mechanism differs from long wavelength mechanism, at 266 nm the damage mechanism occurs through two-photon absorption, whereas at longer wavelengths the two-photon process does not occur [26].

Lenk and Witke (2000). Clarified that nonlinear effect performance depends on three conditions: a high repetition rate, TEM_{oo} beam quality and a high pulse power. They found the use of nonlinear effects makes the precision machining of transparent materials like glass with solid state lasers feasible [5].

Schaffer et al. (2001) suggested using tightly focused femtosecond laser pulses of just 5 nJ, to produce optical breakdown and structural change in bulk transparent materials. Also they studied the morphology of the structures produced by single and multiple laser pulses. At a high repetition rate, multiple pulses produce a structural change dominated by cumulative heating of the material by successive laser pulses. Writing single-mode optical waveguides inside bulk glass was achieved [45].

Schaffer et al. (2001). presented basic mechanisms that lead to laser-induced breakdown and damage. The results indicated that avalanche ionization produces most of the free electrons for large band-gap materials, while photoionization produces a significant fraction of the electron density for small bandgap materials. Also a method for measuring the threshold intensity required to produce breakdown and damage in the bulk was obtained [22].

Du and shi (2003) used very high laser intensities with modern diode pumped solid stat laser having high beam quality and high pulse power, Sub surface engraving of glass was achieved throw nonlinear absorption in transparent media [46].

Shin et al. (2005) implemented to create an image engraved inside crystal and PMMA. Using a Q-switched 2nd harmonic Nd:YAG laser. Laser engraving inside PMMA created image formation better from pure melting process rather than from cracking process inside the crystal. Also they present PMMA as an alternative material to crystal [47].

Mottay et al. (2008) used industrial ultrafast laser system for internal marking and engraving of transparent materials using a diode-pumped femtosecond laser, a high speed scanner, sample handling system and reading device. They analyzed that laser energy in such a short time may lead to two effects first, the light intensity becomes extremely high, allowing ablation of virtually any material. Second, there is no heat dissipation during the interaction process, which becomes essentially a thermal. There was therefore no possibility for micro-cracks or fractures to develop [40].

Alexander A (2014) made a review in damage mechanisms and proposed that the most effective damage mechanism is thermal explosion, impact ionization and photoionization .the impact ionization took place at nanosecond duration range [25].

Verburg et al. (2015) they applied pulse lasers to produce subsurface modifications inside silicon by employing near- to mid-infrared light to achieve subsurface separation. Different wavelengths, pulse durations and pulse energies were tested. It was found that rapid resolidification occurs immediately after sub surface melting of silicon. Lattice defects and transformations to both amorphous silicon and pressure-induced high density silicon phases occurred as a result of the laser irradiation [48].

1.14 The Aim of the work

This work is concerned with:

1. Experimental investigation for the probability of subsurface engraving for two different types of transparent materials BK7 glass and PMMA with nanosecond Nd-YAG laser.

2. Investigate different parameters of the laser and observe the effect of its variation in dots area, shape, surrounding cracks and resolution.

3. Explain the mechanism of sub surface laser engraving that took place.

4. Make a simulation model and compare it with the experimental results.

Chapter Two

Materials and Methods

2.1 Introduction

This chapter introduces the laser systems used for sub surface laser engraving process.

Two systems of Q-switched Nd-YAG laser were used to achieve this process on two different materials BK7 glass and PMMA. For the characterization, transition microscope was used to calculate dots area and depth, UV-VIS, spectrophotometer was also used to find out the material absorbance. Scanning electron microscope was also used to investigate the morphology of the modified area. Computational modeling of the current work cases is also explained.

2.2 Materials

The materials selected in this study are BK7 and PMMA. Both of them are transparent and suitable for this type of application.

2.2.1 Workpiece Dimension

2.2.1.1   Borosilicate crown glass (BK7)

It was imported from (Russian Optics Company); the dimensions of the BK7 glass samples are summarized in Table (2.1).

Table 2.1: BK7 glass characteristics dimensions

Bk7	Length (mm)	Width (mm)	Thickness (mm)	nots
Type 1	100	50	10	Polished from the interior and posterior sides
Type 2	20	20	15	All sides are polished

2.2.1.2 Poly Methyl Methacrylate Polymer (PMMA)

The PMMA used in our research is commercially made by Asia poly industrial company also known as acrylic glass.

The dimensions of PMMA sample was (50 x50x10) mm no polishing was done to the PMMA, Just surface cleaning by distilled water.

2.2.2 Material's specifications

2.2.2.1 BK7 glass

The physical and mechanical properties of BK7 glass are presented in Table 2.2

Table 2.2 The physical and mechanical properties of BK7 glass (appendix A)

Parameters	BK7
Melting Point ($°K$)	830
Thermal Conductivity ($W\ m^{-1}\ K^{-1}$)	1.114
Thermal Expansion (K^{-1})	7.1×10^{-6}
Hardness (knoop)	610
Specific Heat Capacity ($J\ Kg^{-1}\ K^{-1}$)	858
Density (Kg/m^{3})	2.51

2.2.2.2 PMMA

The mechanical and thermal properties of this material are listed in table 2.3

Table 2.3 the physical and mechanical properties of PMMA (appendix B)

Parameter	PMMA
Melting Point (°K)	423
Thermal Conductivity (W m^{-1} K^{-1})	0.19
Specific Heat Capacity (J/g.°C)	1.46
Density (kg/m^{3})	1.19
Hardness (shor D)	86

2.3 Laser sources:

The laser sources that were used in this work are:

2.3.1 First source

Lightmed Corporation SYL9000 system, Korean made Q-switched Nd:YAG laser (in the Institute of Laser for Postgraduate Studies / University of Baghdad) as shown in figure 2.1

 The laser wavelength is 1064nm, energy is from 0.2 mJ to 10 mJ in single pulse mode, pulse width 4ns, repetition rate is1 Hz and spot size is 100μm, and the laser is supplied with (CW) diode laser aiming beam.
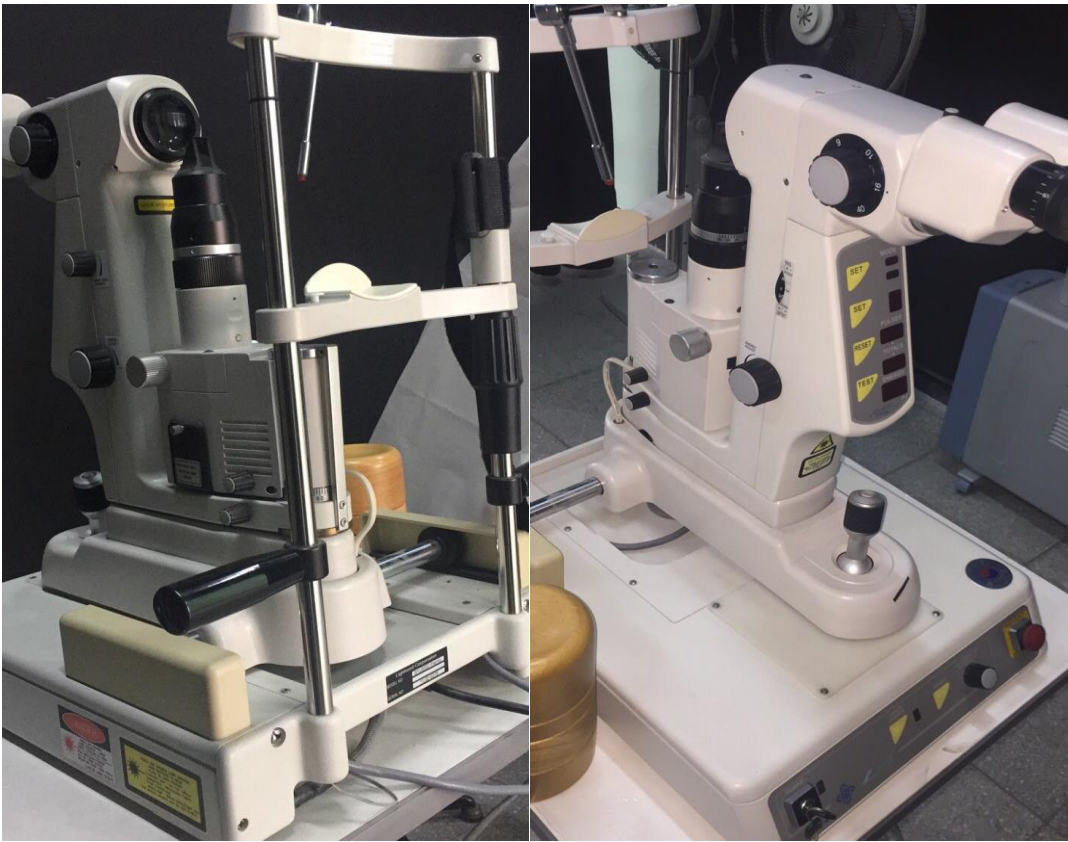
Figure 2.1 Lightmed SYL9000 Nd:YAG laser

2.3.2. Second source

Q-switched Nd:YAG laser model HF-304 (Diamond -288-China made) was used in this thesis at the Institute of Laser for Postgraduate Studies / University of Baghdad as shown in figure 2.2.

This laser has two output wavelengths,1064 nm and second harmonic generation 532 nm,10 ns pulse duration, maximum energy 1000 mJ and 1 to 6 Hz frequency and focusing lens with 32mm focal length and 200 μm spot size.

The second harmonic wavelength (532 nm) is generated by Potassium titanyl phosphate (KTiOPO4) KTP crystal.
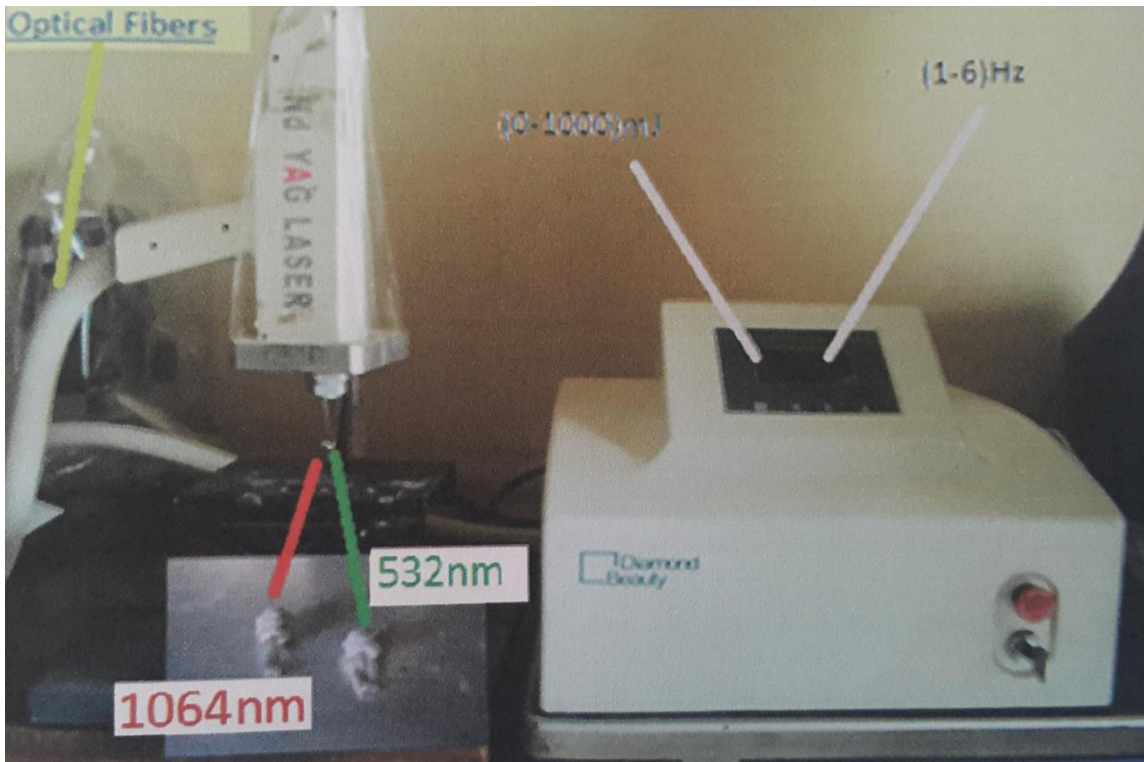
Figure 2.2 HF-304 Diamond Q-switched Nd:YAG laser

2.4 Experiment procedure

2.4.1 Fixing the sample

To fix the sample, manual stage was used which has incremental spacing of 1 mm as shown in figure 2.3 ,the manual stage binds by tall prop to hold the work piece in front of the first laser system. The manual stage offered easy control of the depth of laser focus inside the material, which is an important part of this study, in order to study the effect of focal position shifting.
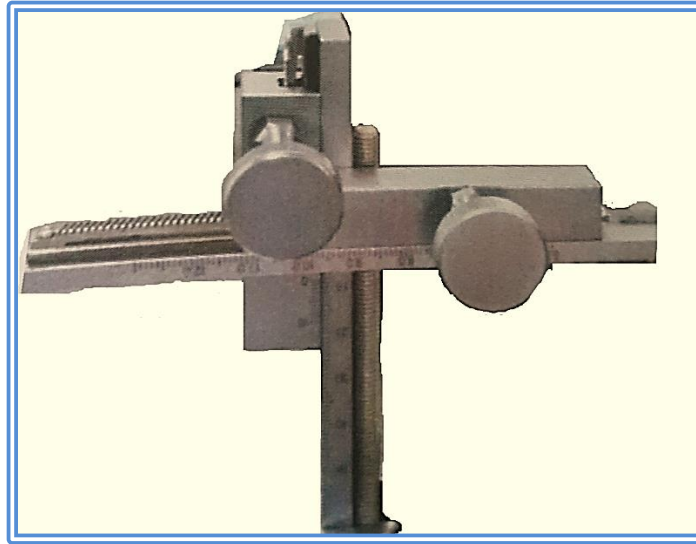
Figure 2.3 The manual stage

2.4.2 Moving the sample

For engraving an image which represent a matrix of dotes inside the sample, CNC work station must be used to complete this process.

Homemade 2D CNC work station with adjustable speed was designed for this purpose, the sample was fixed on the CNC workstation as shown in Figure 2.4

Figure 2.4 Two dimensions Computer Numerical Control (CNC) work station

2.4.3 Moving the Laser

HF-304 Diamond Q-Switched Nd: YAG laser handpiece was fixed on the CO_2 laser CNC work station at the Institute of Laser for Postgraduate Studies/University of Baghdad to insure well controlled feeding as shown in Figure 2.5

Figure 2.5 Diamond Q-Switched Nd: YAG laser fixed on the CO_2 laser CNC work station

2.4.4 Experiment processes

At the beginning it was important to study the effect of the laser beam energy variation on both materials BK7 glass and PMMA and also to observe the influence of focal plane position changing of the laser inside the two materials.

It was also important to study the effect of single, double and triple pulses on the same spot site.

Several parameters such as frequency, feed of the CNC work station and pulse repetition rate were taken in account to make sure that the best resolution of images were achieved.

The feed rate of the CNC that used is 100(1.56mm/s), 200(2.5mm/s), 300(4.3mm/s), 400(5.8mm/s), 500(7.7mm/s) and 600(8.5mm/s).

2.5 Tests

2.5.1 Microscopic inspection

Sub surface laser engraving results were inspected by Olympus transmission microscope, U-YVO-63XC model with CCD camera type Olympus model DP72 which was connected to a computer.

The microscope lens that was used has 10X magnification power to investigate the samples.

The sub surface laser engraving effects (dots) shape, depth and area were characterized by microscope. After all, the best results were diagnosed in order to use it in this application.

2.5.2 Absorption measurement

UV-VIS spectrophotometer type Shimadzu 1800 was used. This device has very high resolution, it's wavelength range is from 90 nm to 1100nm, where the laser being used to perform the experiments within this range .

The material was examined to identify the absorptivity of material at both 532 nm and 1064nm wavelengths.

2.5.3 Scanning Electron Microscope (SEM)

Scanning electron microscope studies the morphological changes and analyzes the material structure. This device (FEI model Inspect S50) exists in AL-Nahrain University /Department of Physics .

2.5.4 Laser energy monitors

Laser Energy Monitors was used for calibrating the laser beam energy, This monitor is Gentec-ε, maestro model.

The result of calibration of HF-304 Diamond Q-switched Nd:YAG laser for the wavelength 1064 nm and 532 nm is depicted in Figure (2.6)
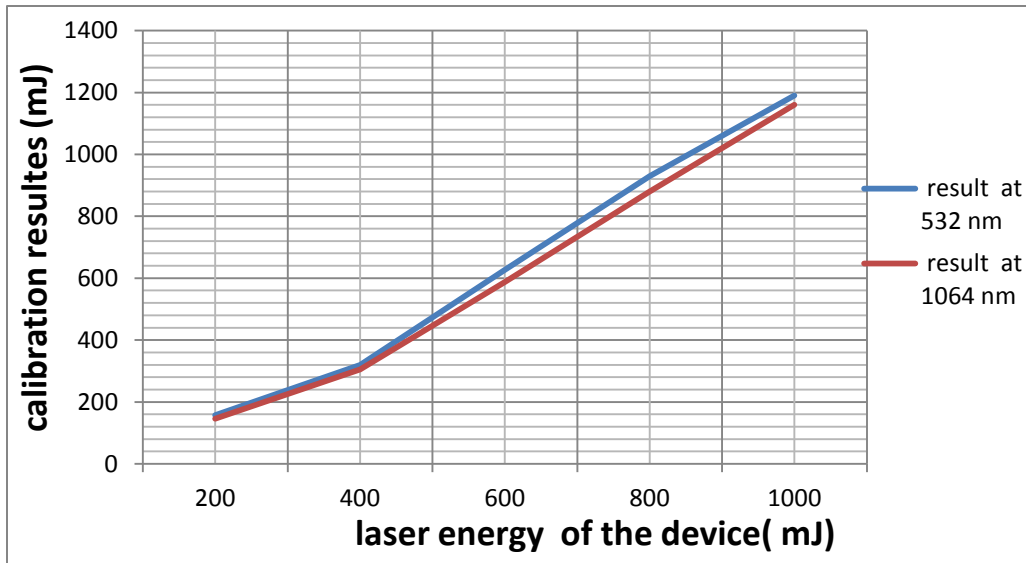

Figure 2.6 Calibration results of HF-304 Diamond Q-switched Nd:YAG laser for both wavelengths 1064 nm and 532 nm.

2.6 Computational method

COMSOL Multiphysics 4.3 b package program was used to simulate the laser interaction with BK7 glass. The effect of single pulse of laser is to create microhole inside the material, then the diameter and depth were intended to be measured.

2.6.1 Geometry and mesh distribution

The physics type that was selected to perform this work is heat transfer. The BK7 work piece dimensions were 100x50x10cm. The heat transfer equation that previously explained in chapter one was used in this simulation, then the material were selected from the material library of the COMSOL program, the work

accomplished at the room temperature. There are different sizes of the mesh, the shape of the mesh may be triangular or rectangular with all the model geometry meshed into small size spaces as shown in figure (2.7).
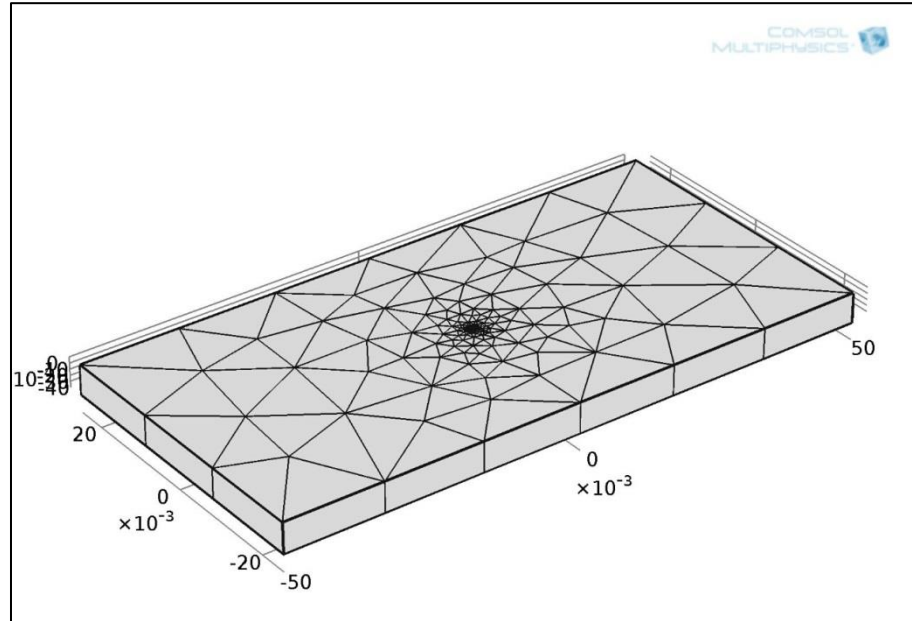

Figure 2.7 The geometry of BK7 glass after meshing

Chapter Three

Results
and
Discussion

3.1 Introduction

This chapter presents and discusses the results of the experimental work of the subsurface engraving by nanosecond Q-switched Nd-YAG laser (532 nm and 1064 nm in wavelength) interaction with two transparent materials, BK7 and PMMA. As it was mentioned in Chapter One laser engraving inside the sample consists of many dots gathered to make a mesh of dots to create a certain shape or write a certain word inside the work piece ,the distribution of these dots decide the final result (inscription, pictures ,..).

Simulation model has been done by COMSOL Multiphysics and the results obtained from the simulation Compared with experimental results.

3.2 Experimental results

The effect of variable laser parameters such as laser energy, focal plane position, feed rate of the CNC workstation, laser wavelength ,as well as multiple pulses effect on the same spot, were examined for both materials BK7 and PMMA.

3.2.1 Laser energy effect

The effect of laser pulse energy in subsurface engraving process was examined for both BK7 and PMMA in order to perform a comparison between them. The energies 1,3,5,7and 10 mJ were used to investigate the energy effect on the damaged central area (dots), at 1064nm laser wavelength, 100 μm spot dimeter and pulse duration 4ns .The depth of focusing of the laser beam inside the sample is the same for both materials ,the area was measured for the central damage of the dots .

Figure (3.1) shows the effect of energy on the dots area for both materials.

Table (3.2) shows the dots shapes modifications as the laser energy increased for both materials.

Table 3.1 The laser energy effect on the dots area for BK7 and PMMA.

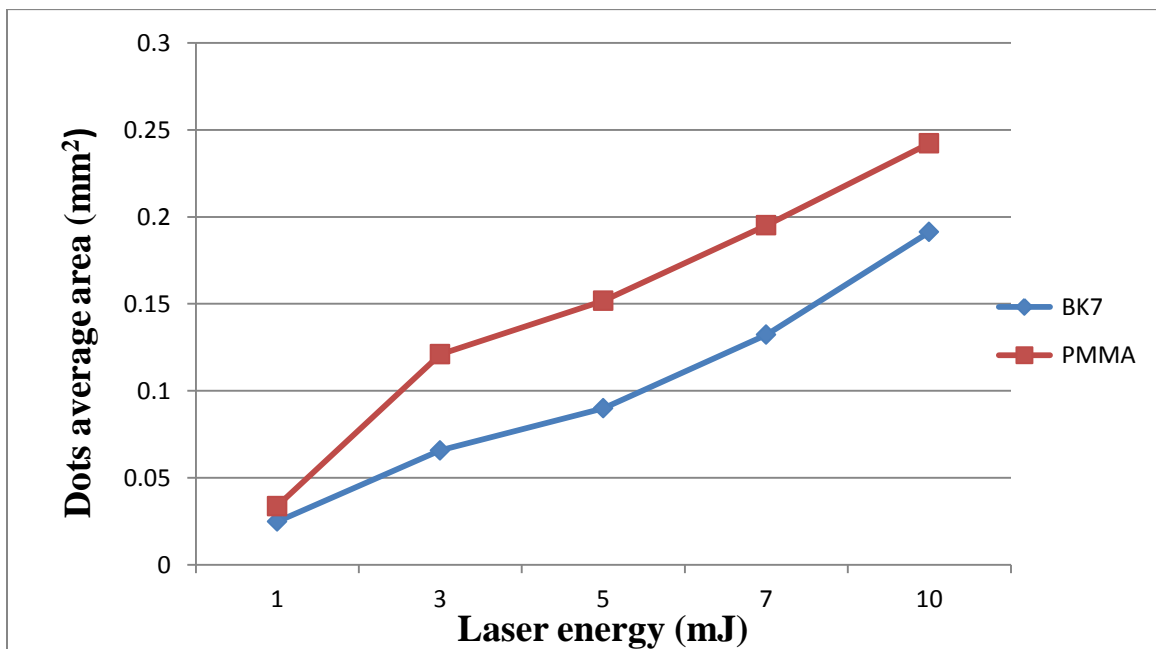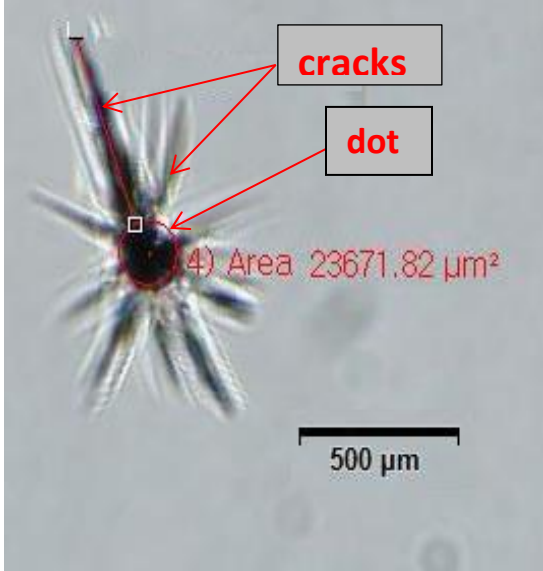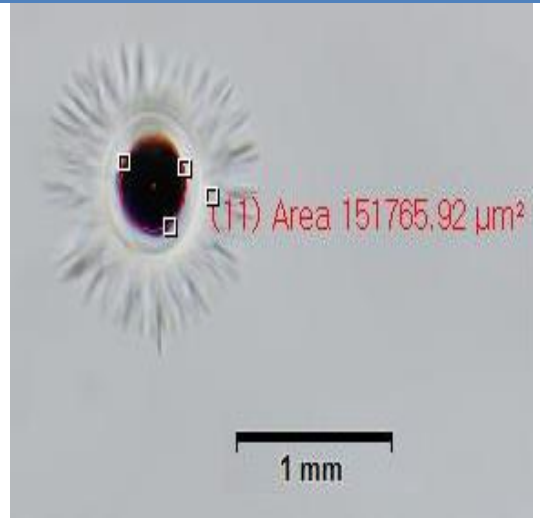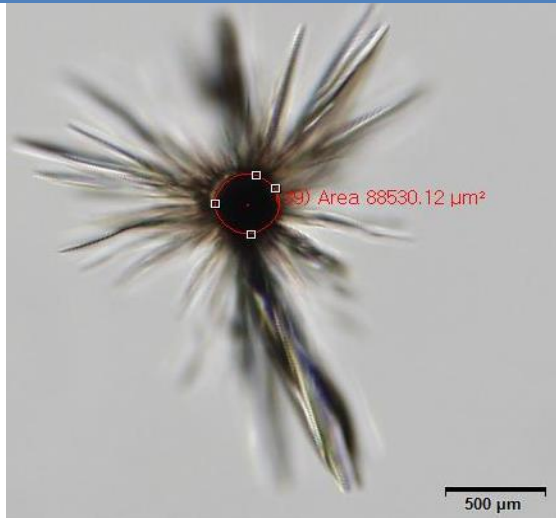| Laser energy (mJ)	Dots area BK7(mm^2)	Dots area PMMA(mm^2)
1	0.024858	0.033781
3	0.065773	0.121021
5	0.089930	0.151765
7	0.132282	0.195223
10	0.191357	0.242300

Figure 3.1 Relation between the dots average area and the laser energy for BK7 and PMMA at 1064 wavelength.

Table 3.2 Microscopic images of the dots modification for BK7 and PMMA at different energies.

Energy	BK7 glass	PMMA
1 mJ		
3 mJ		

5 mJ

(39) Area 88530.12 µm²

(11) Area 151765.92 µm²

500 µm

1 mm

7 mJ

(32) Area 129674.99 µm²

(70) Area 199692.00 µm²

500 µm

1 mm

10mJ

(128) Area 203394.62 µm²

(127) Area ~

(97) Area 254440.89 µm²

500 µm
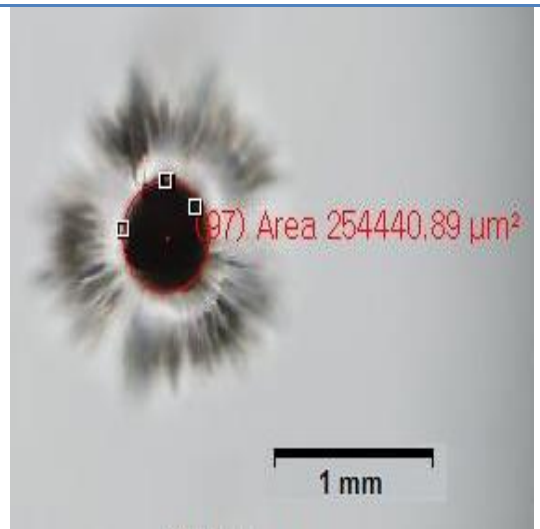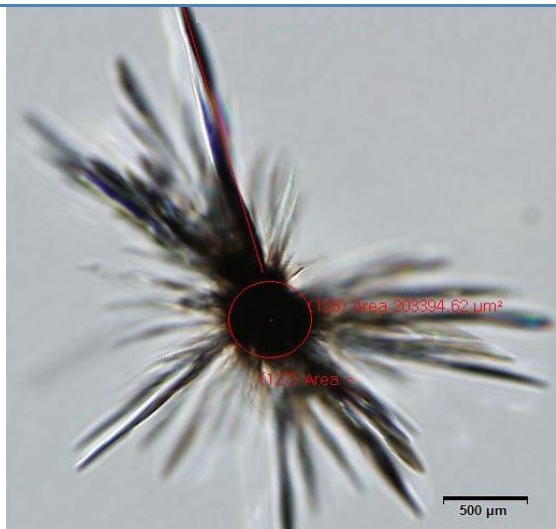
1 mm
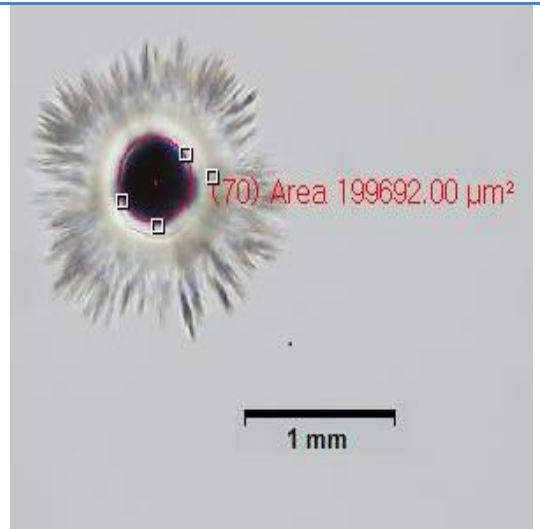
As shown in table 3.2 dots area increase with increasing the laser energy. Dots in BK7 almost have the same shapes, with approximately similar length of surrounding cracks.

In PMMA, laser does not induce cracks in general, except in some cases, and these cracks increase in incidence as the energy of laser increase as shown in Figure (3.2 a and b), in which both images are for PMMA at the same energy

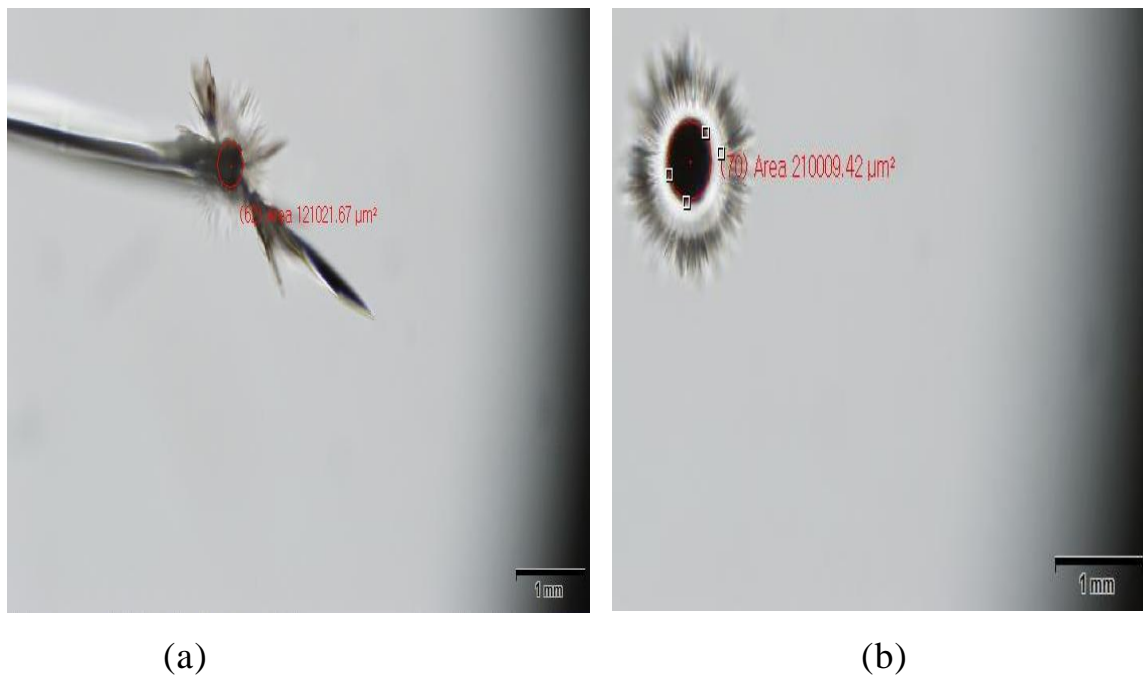(a)   (b)

Figure 3.2 Microscopic images of PMMA dots at 6.4 mj (a) with cracks (b) without cracks.

In spite of the large number of surrounding crakes in Bk7 glass, dots engraved in the BK7 have better distribution than those in the PMMA; this attributed to the regularity of BK7 cracks and the clarity of BK7comparied to PMMA.

3.2.2 Focal position effect

Focal plane position (f.p.p) is one of the most effective factors, to ensure the maximum power density during the machining process; the focal plane is normally positioned on the sample surface, it's called zero focal plane position. If focal plane position lies under the surface then it is called negative focal plane position, which is the concern of this work.

Different negative focal plane positions were examined with different laser energies in order to demonstrate the modification in the dots area as the negative focal position installed deeper inside the workpiece.

Nd-YAG laser with fundamental wavelength (1064nm) was used, with 4ns pulse duration and spot diameter of 100 μm. For the BK7 glass the depth of the dots from the workpiece surface increase incrementally from (-2 to -10) mm and the laser energy varies from (2 - 8.5) mJ as shown in Table (3.3) Figure (3.3) Figure (3.4).

Table 3.3 BK7 glass results of focal position effect in dots area in different laser energies.

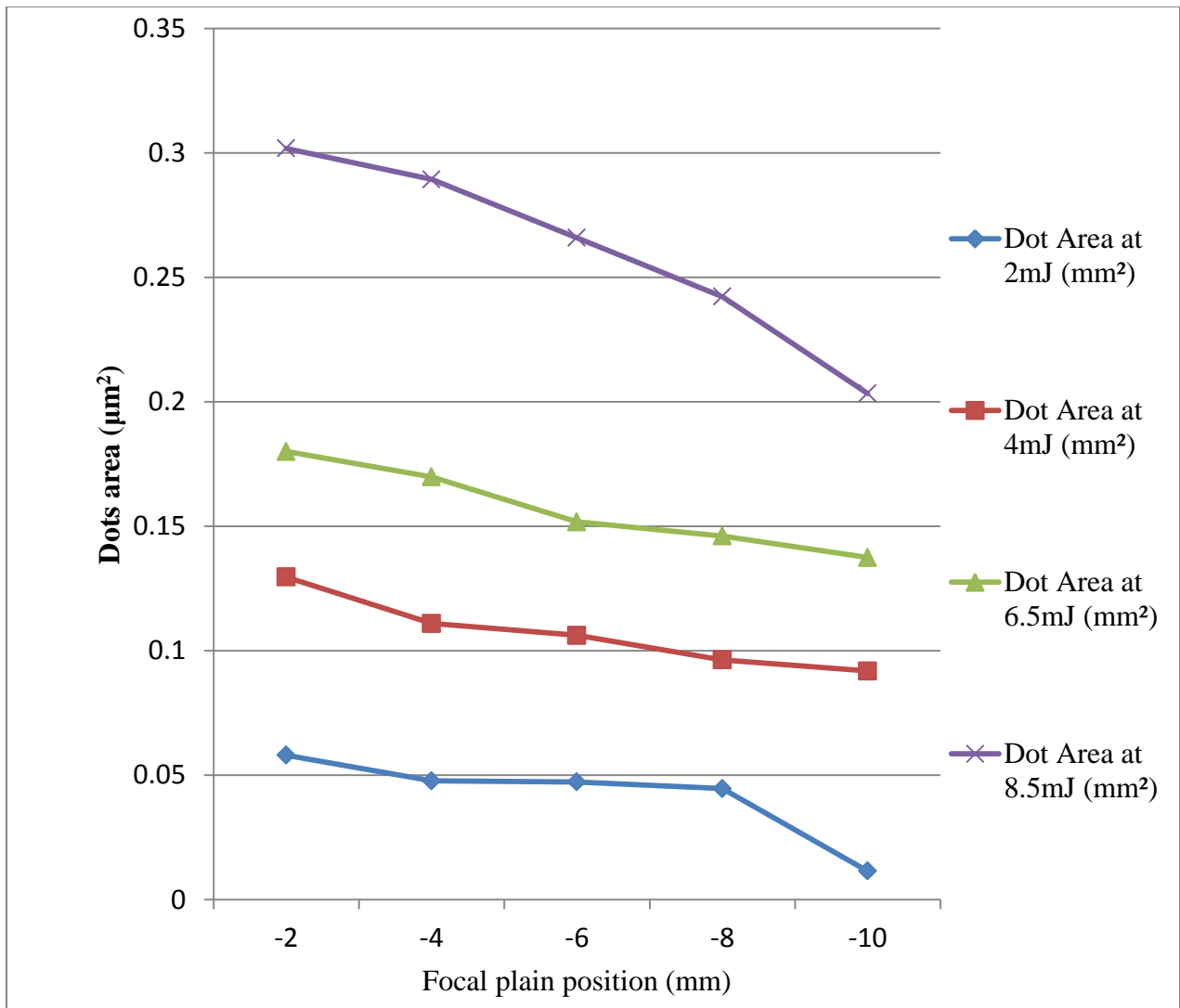| Focal plane position (mm)	Dot Area at 2mJ (mm²)	Dot Area at 4mJ (mm²)	Dot Area at 6.5mJ (mm²)	Dot Area at 8.5mJ (mm²)
-2	0.058077	0.129675	0.180055	0.301867
-4	0.047760	0.110995	0.169904	0.289387
-6	0.047343	0.106211	0.151765	0.265923
-8	0.044639	0.096351	0.146149	0.242293
-10	0.011524	0.091899	0.137496	0.203394

Figure 3.3 The relation between focal position and dots area as a function of energy in BK7 glass.

Figure (3.3) shows that the focal position plays a key role in the dots area formation, dots area decreases as the focal position becomes deeper inside BK7, the changes in the dots area becomes more acute as the laser energy used increases, which attributed to the energy losses inside the material.
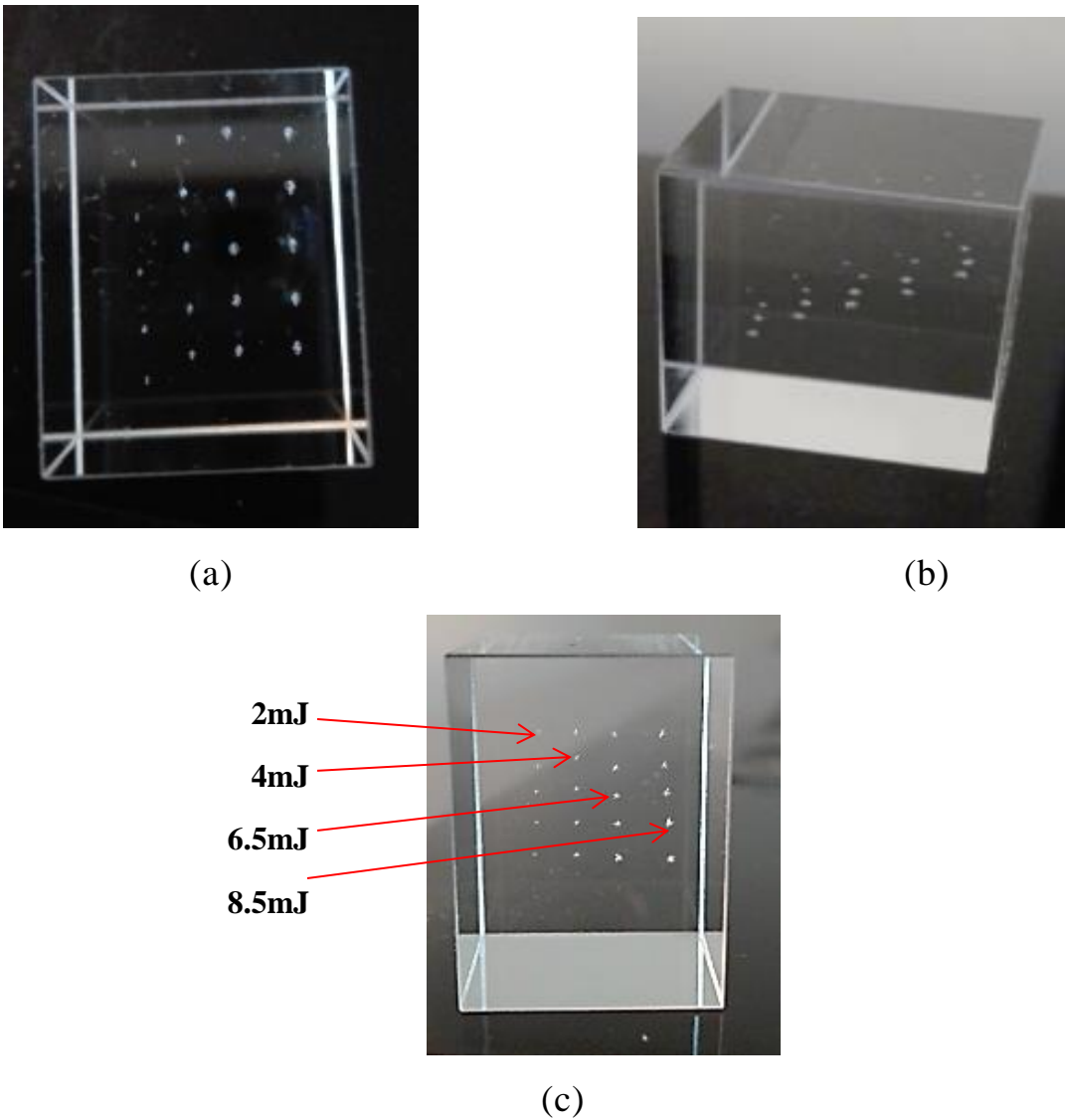
(a)

(b)

(c)

Figure 3.4 Images showing dots in the BK7 at different focal plane positions with different energies (a) top view (b) side view (c) front view.

The same laser was used for PMMA to investigate the focal plane position effect. The depth of the dots from the workpiece surface increases incrementally from (-1 to -5) mm and the laser energy varies from (3.5 -8)mJ as shown in Table (3.4).

Table 3.4 PMMA results of focal position effect in dots area in different laser energies.

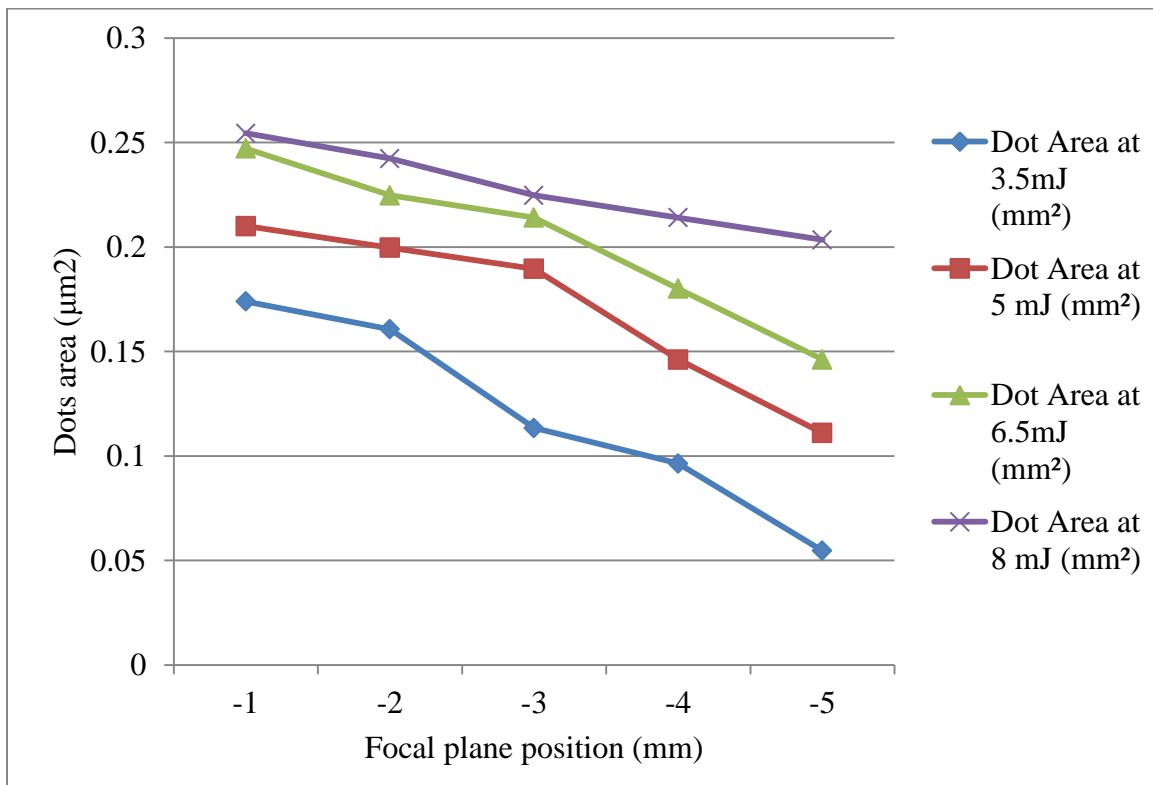| Focal plane position (mm)	Dot Area at 3.5mJ (mm²)	Dot Area at 5 mJ (mm²)	Dot Area at 6.5mJ (mm²)	Dot Area at 8 mJ (mm²)
-1	0.173940	0.210009	0.247160	0.254440
-2	0.160585	0.199692	0.224695	0.242293
-3	0.113366	0.189547	0.214044	0.224695
-4	0.096351	0.146149	0.180055	0.214044
-5	0.054624	0.110995	0.146149	0.203394

Figure 3.5 The relation between the focal position and dots area as a function of energy in PMMA.

Figure (3.5) illustrates that the focal position has considerable effect in the dots area. Dots area decrease as the focal position become deeper in the PMMA sample. The changes in the dots area become less acute as the laser energy increase, which attributed to the losses of energy and inhomogeneity of PMMA.

3.2.3 Laser wavelength effect

The wavelength is an important parameter that affects the dots area.

Figure (3.6a) shows the experimental results of the absorptivity of BK7 which are 0.036 for 1064nm and 0.037 for 532nm; in spite of the quality of the resulted values of the absorptivity the two employed wavelengths affect the dots area differently.

Figure (3.6b) shows the experimental results for the absorptivity of PMMA at 1064 nm and 532nm equals to1.92 and 1.97 respectively.
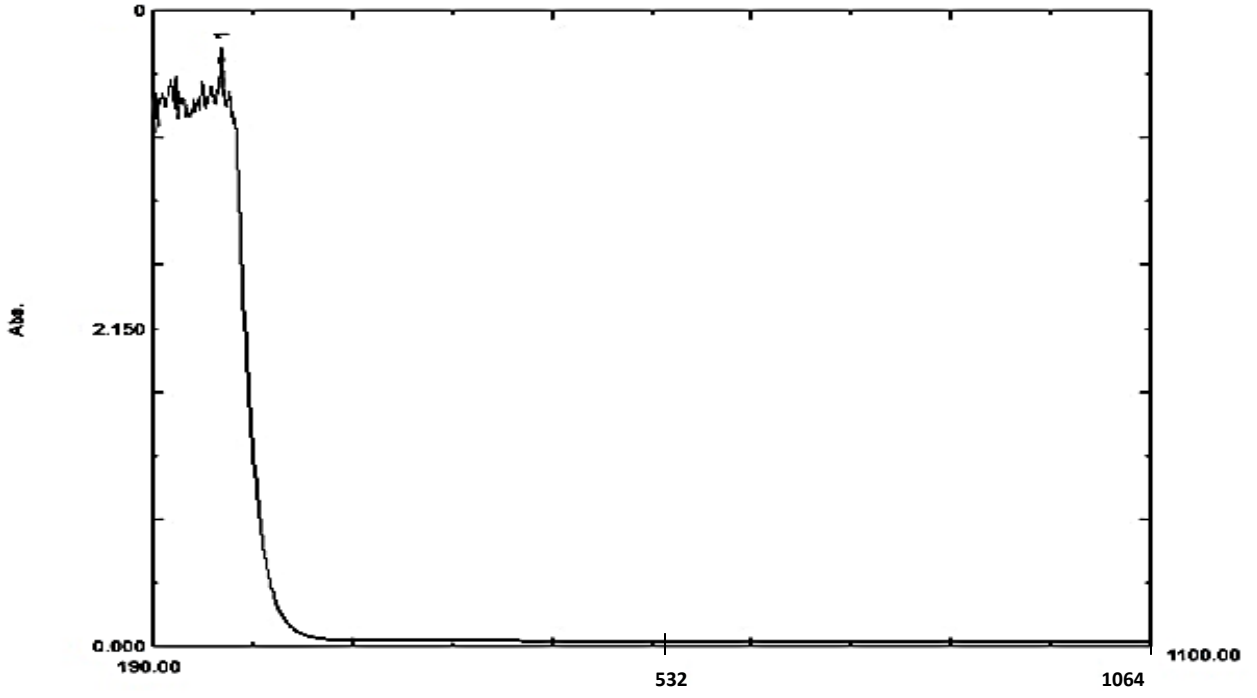
(a)
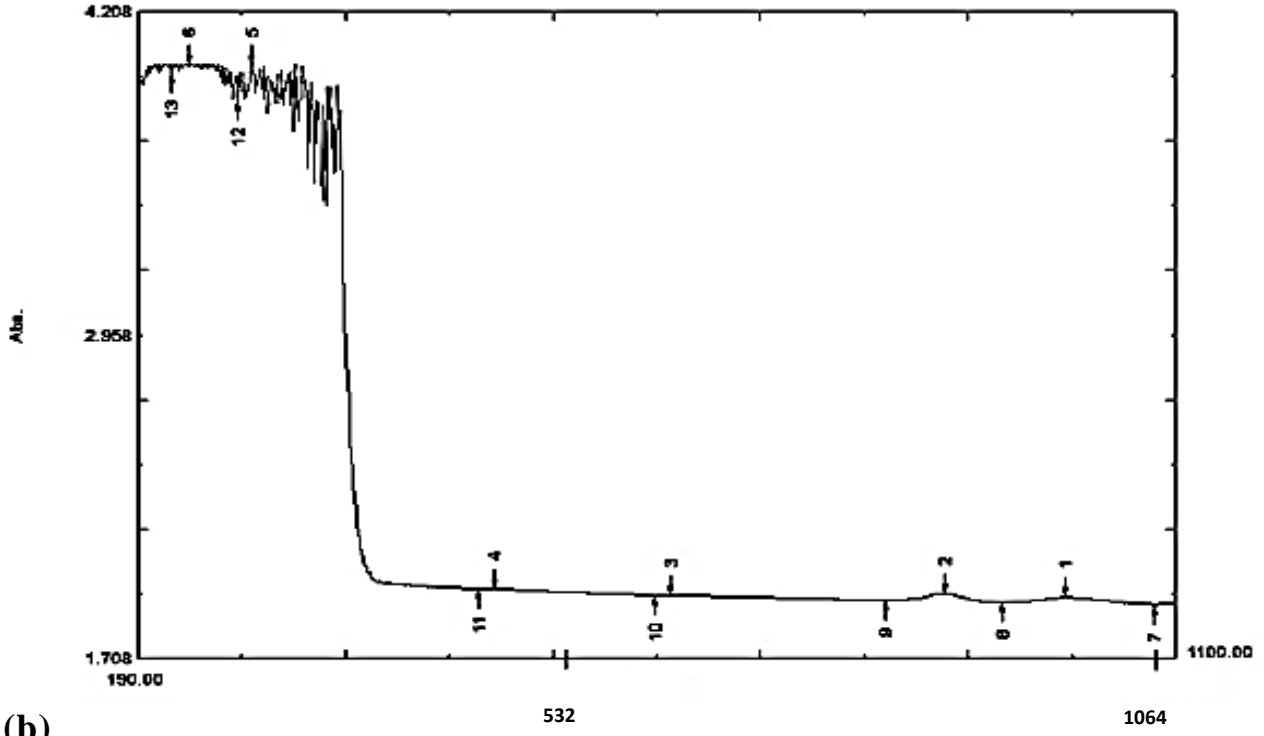
(b)

Figure 3.6 Absorptivity at range from (190-1100)nm for a. of BK7 glass
b. PMMA.

In this experiment both wavelengths were used at different laser energies graduated from (240 -480) mJ and the effect on the dots area had been examined, as shown in the Figure (3.7).
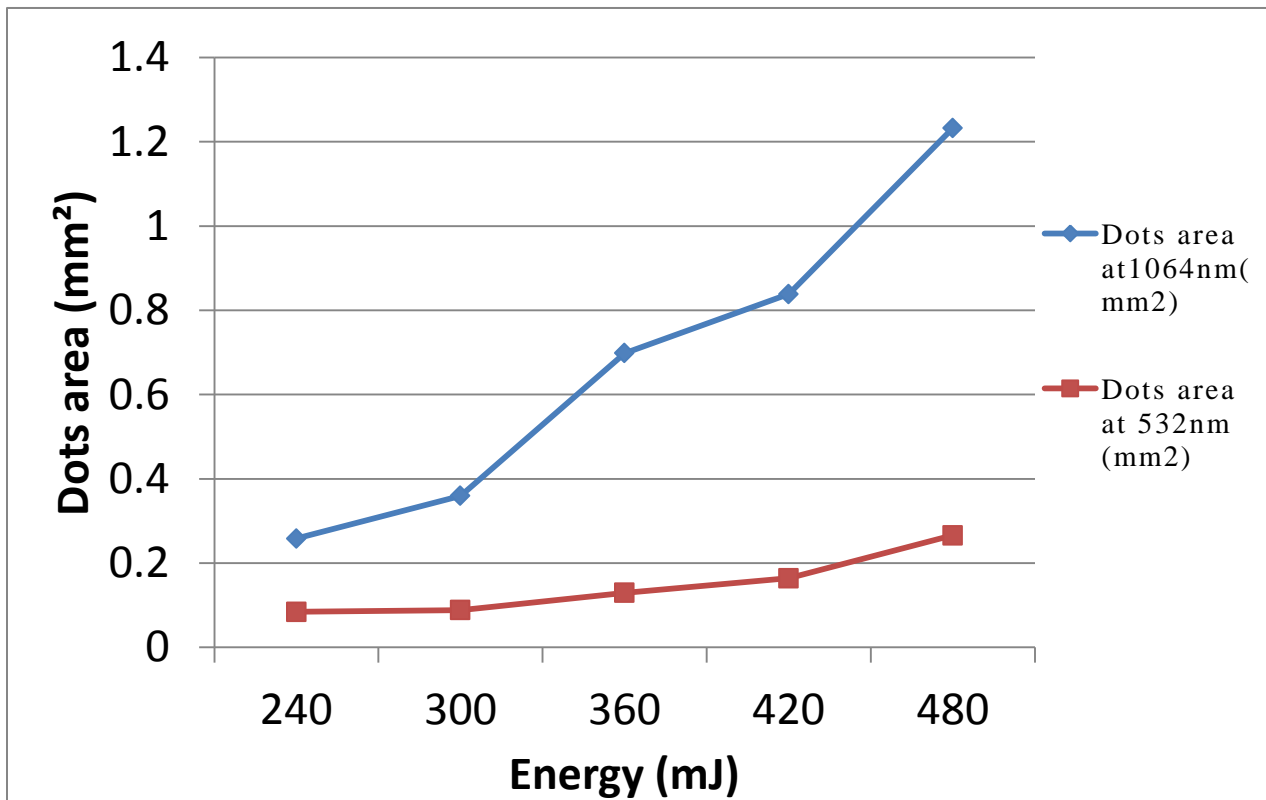
Figure 3.7 The relation between the energy and dots area at two wavelengths 1064nm and 532 nm in BK7.

From the figure (3.7) we can observe a significant difference in the dot size induced by 532 nm laser which is less than that induced by 1064 nm laser, this results coincide with HU in 2012 [49], who suggest formation of plasma and the interaction force among the adjacent plasma obstructs the plasma expansion.

The dots produced at both two wavelengths are similar in shape and morphology but are different in dots surface area.

Dots area for PMMA at 532nm wavelength cannot be measured by microscope due to the disfiguration of the dots with no define borders for the dots due to the large spot size and high energy range of laser as can be seen in Figure (3.8), but it still obvious that 1064nm wavelength causes effect larger than 532nm.

Figure 3.8 Laser effect on PMMA at wavelength 532 nm.

3.2.4 Number of pulses effect

This part of the work examines the effect of increasing the number of laser pulses (on the same spot site) on dots surface area, depth of penetration and shape in BK7.

Several energies were used from (1.5-7mJ) with constant negative focal plane position while the number of pulses increased gradually from (1-4) pulses.

3.2.4.1 Number of pulses effect on surface area of the dots

There is obvious change in dots area as the number of laser pulses increased, as shown in Table (3.5) and Figure (3.9).

The increases in the number of pulses leads to increases in the dots area and also enhancing the surrounding cracks growth, so it is not recommended to use more than one pulse at the same site due to the possibility of over lapping with the adjacent dots.

Table 3.5 BK7 results of number of pulses effect on dots area at different energies.

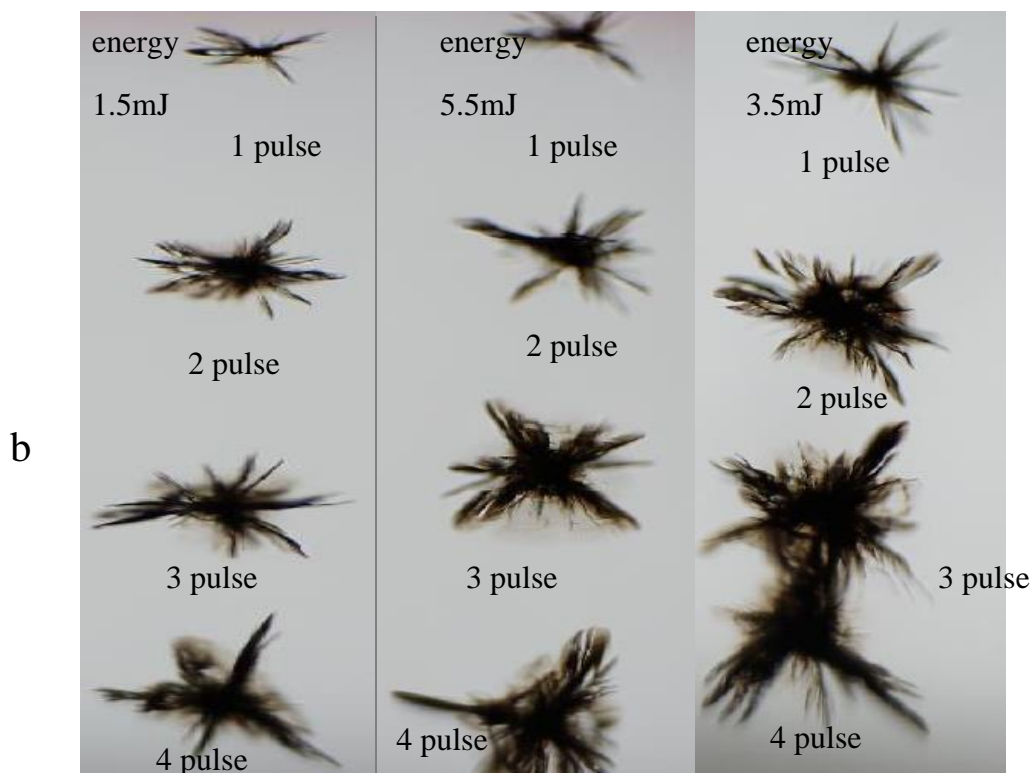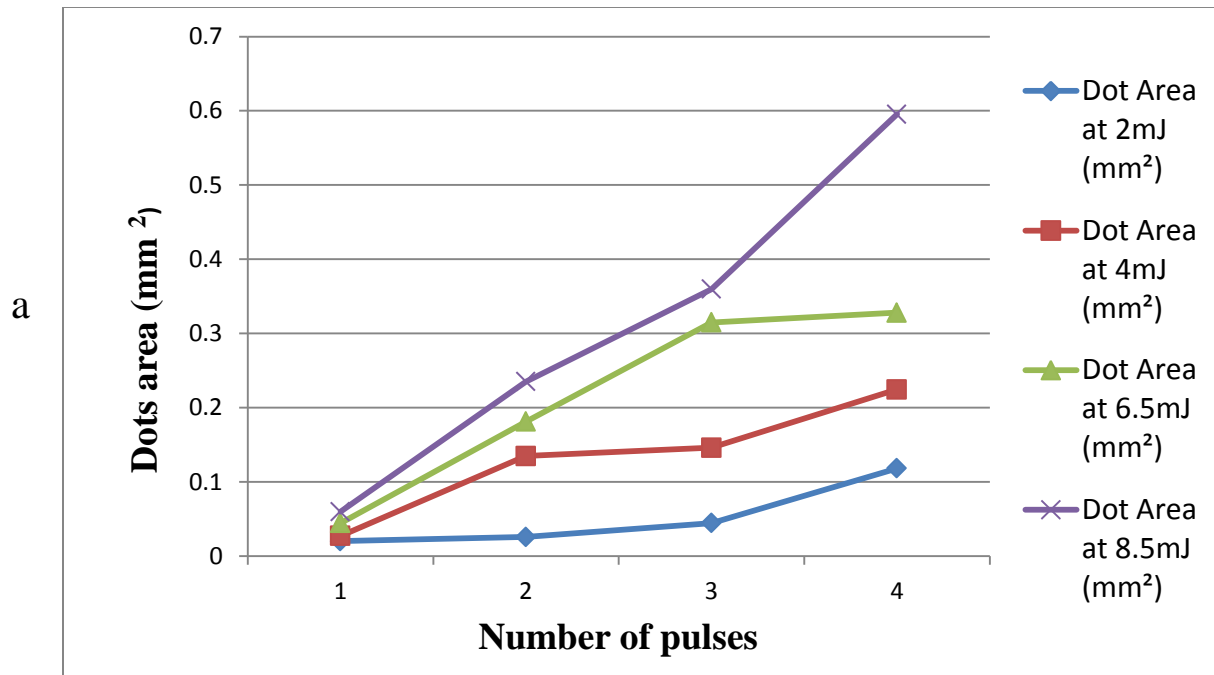| Number of pulses	Dots area at 1.5 mJ	Dots area at 3.5 mJ	Dots area at 5.5 mJ	Dots area at 7mJ
1	0.020343	0.02733	0.04464	0.05995
2	0.025959	0.13495	0.181317	0.235178
3	0.044639	0.14615	0.315014	0.359653
4	0.1183	0.224695	0.328	0.59545

Figure 3.9 a. Relation between the number of laser pulses and dots area at different energies for BK7.**b**.microscopic images for the area modification as the number of pulses increased.

3.2.4.2 Number of pulses effect on the dots penetration depth

The penetration depth of the dots is affected by increasing the number of laser pulses. Figures (3.10 a and b) illustrates the relation between the number of pulse and depth of penetration.

a

b

Figure 3.10   a. Relation between the number of pulses and the dots penetration depth .**b**. microscopic images of the multiple pulses effect.
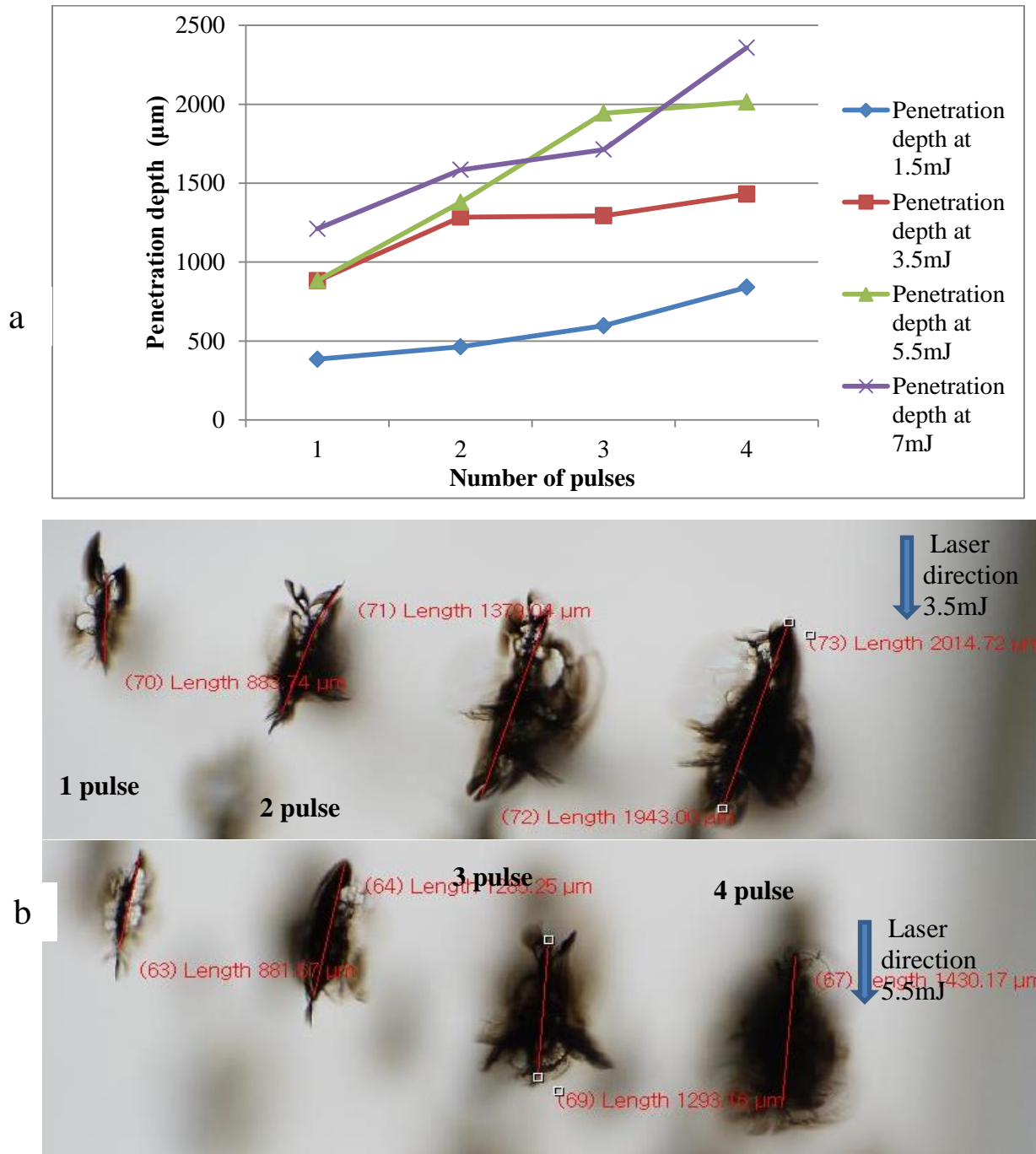
The side view of the affected area illustrates the increase in the penetration depth as the number of pulses increases and becomes more conical in shape.

As it is known when the dot is formed from the first shot, cracks are generated around the dots, increasing the number of pulses in the same point makes the cracks spread and expand due to the additional energy delivered by every single pulse so it is not recommended to use the multi pulse technique.

3.2.5 Feed rate effect

The feed rate is the speed of the CNC work station during the process of SSLE. It has a main effect on the resulting model resolution because it manages the number of dots per unit area of engraving. The increase in the number of the dots per unit area (dots density) –with limits- enhance the model resolution, while decreasing the number of the dots per unit area result in low resolution images as clarified in figure (3.11).
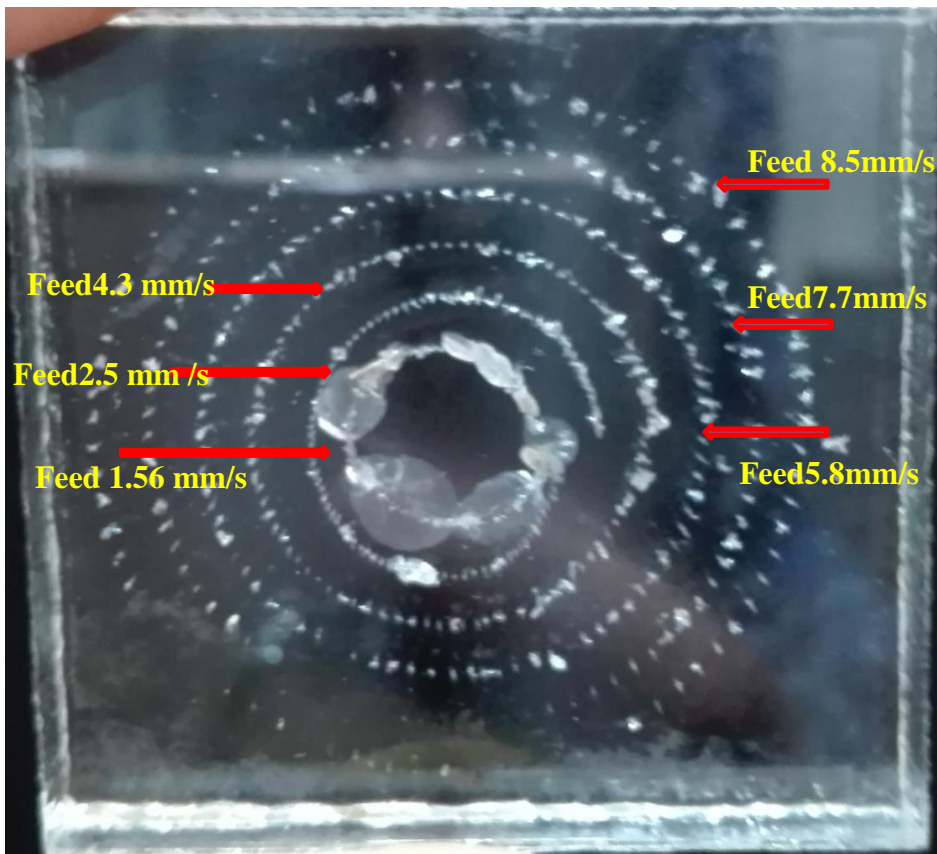

Figure 3.11 Difference in resolution while increasing the feed rate of PMMA.

Nd-YAG laser of 532 nm wavelength was used for this application, the energy is fixed at 360mJ and the pulse repetition rate is 6Hz, different feed rates were used ranging from (1.56-8.5) mm/s in order to investigate the feed rate influence on the sample.

When the feed rate increases it produce low resolution images, while decreasing the feed rate produces high resolution image. The best results were obtained at the feed rate 2.5 mm/s and 4.3 mm/s due to the suitable spacing between the dots. At feed 1.56 mm/s dots overlapping had occurred, this lead to distortion of the model (circle) with indistinct borders.

In order to examine the effect of changing the energy while the feed rate is fixed, BK7sample was engraved using different energies ranging from (200 to 900) mJ with feed rate (5.8 mm/s), wavelength (532 nm), constant pulse repetition rate (6Hz), as shown in Figure (3.12). The engraved line has low clarity at energies 200 and 300mJ and had high distortion at energies 900and 1000mJ so there are no benefits from the increasing the energy with fixed feed rate.
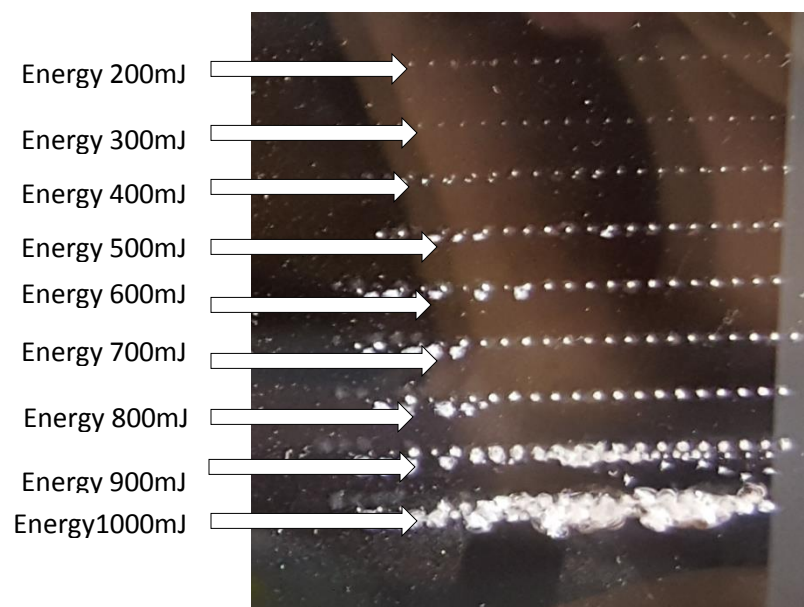

Figure 3.12 Energy effect on SSLE with fixed feed rate for BK7.

Figure (3.13) shows two BK7 models and Figure (3.14) shows two PMMA models that are engraved with fixed energy, pules repetition rate and feed rate (200mJ, 2H , 2.5mm/s) respectively, but at two different wavelengths 1064nm and 532nm.
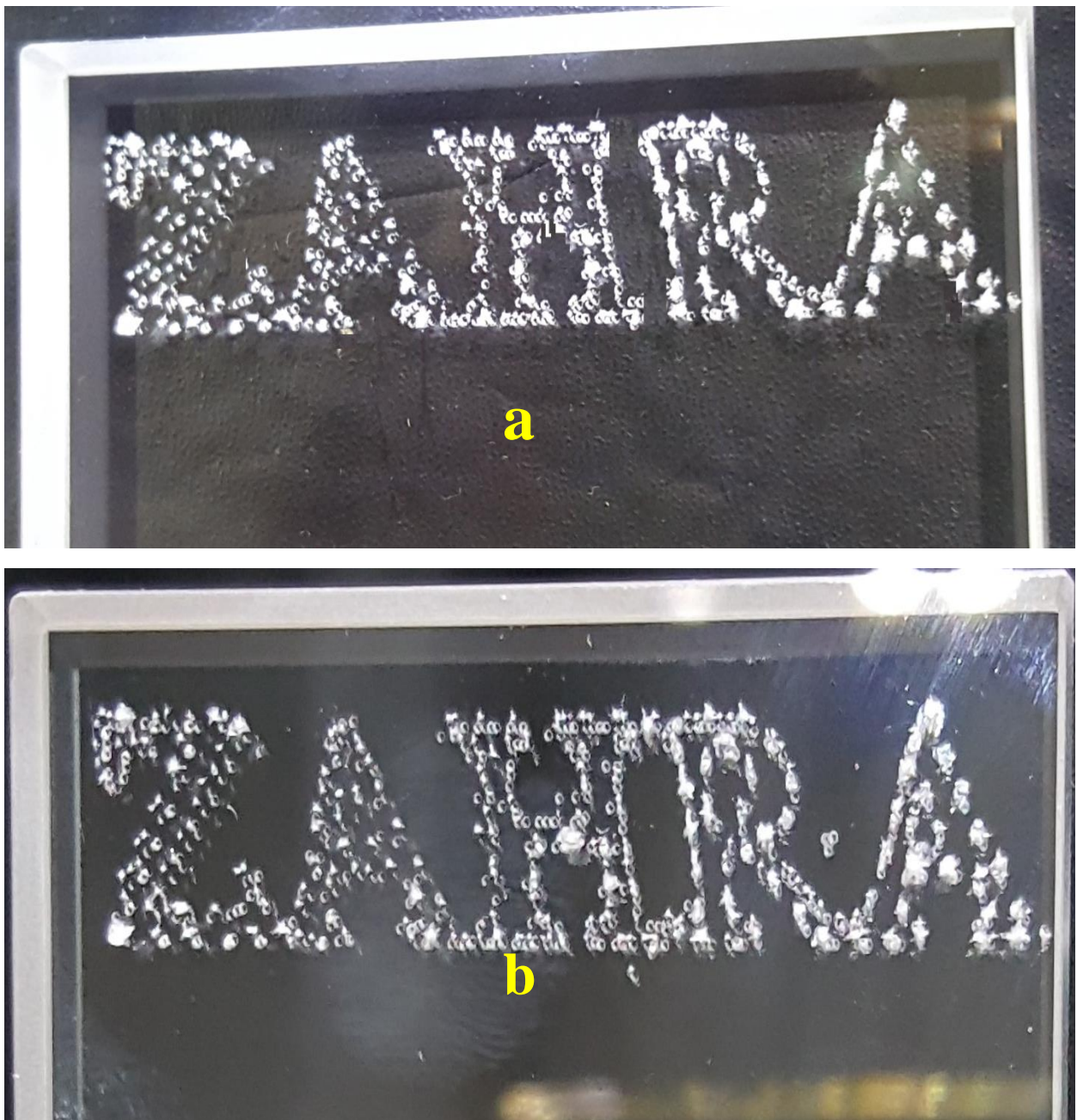

Figure (3.13) BK7 Sub surface laser engraving model at a.532 nm. b. 1064nm

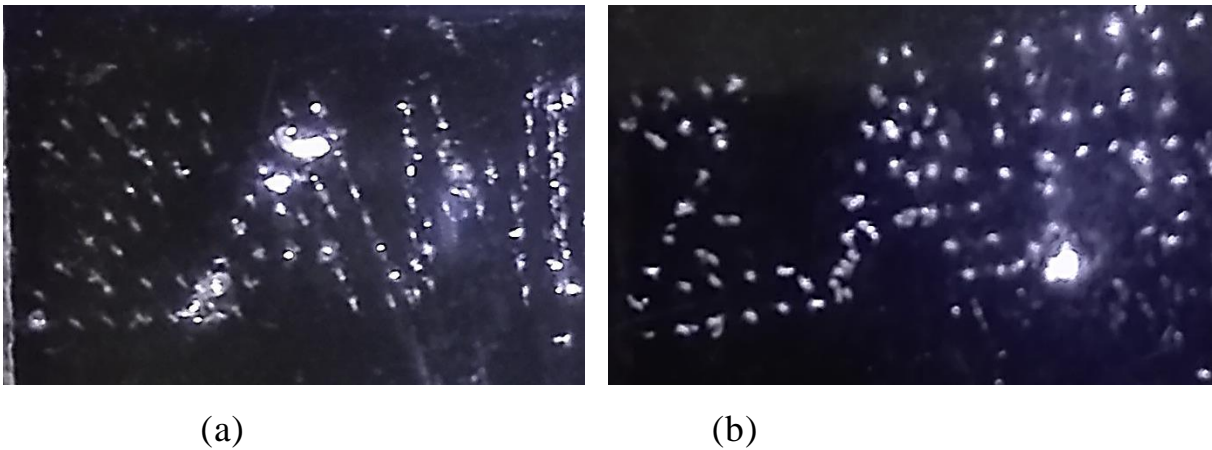(a)   (b)

Figure 3.14 PMMA Sub surface laser engraving model at a.532 nm.

 b.1064 nm.

For both BK7 and PMMA, the change in the wavelength affects the image resolution due to the change in dots area and the surrounding cracks. Model of 2nd harmonic wavelength of Nd-YAG (532 nm) seems to be better than 1064 nm; because the dots are more uniform and the surrounding crakes in 532 nm wavelength are less than in 1064 nm.

Also, the BK7 is still more suitable than the PMMA for this type of application, due to the difference in materials nature, high transparency of the BK7 and its dots is more uniform.

3.2.6 Pulse repetition rate effect

In SSLE pulse repetition rate affect the resolution of the sample, with fixed feed rate of (4.3 mm/s), fixed wavelength of 532 nm; the effect of changing pulse repetition rate ranging a from 1Hz to 6Hz had been examined at three different energy (360,460and560)mJ .

Figure (3.15) illustrates the difference in the resolution of the letter (L) with changing pulse repetition rate values. Pulse repetition rate changing with using 3 fixed energies had significant effect on the resolution; pulse repetition rate 4 and 5Hz at 360mJ produce the best results, due to suitable spacing, dots uniformity and the image clarity.
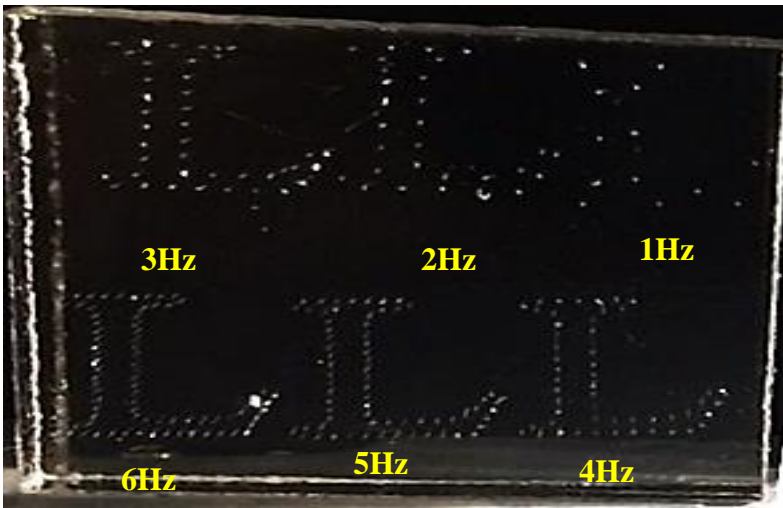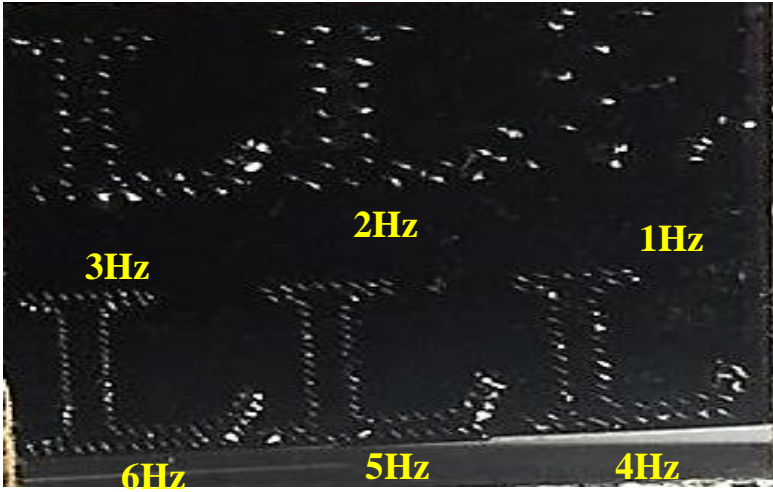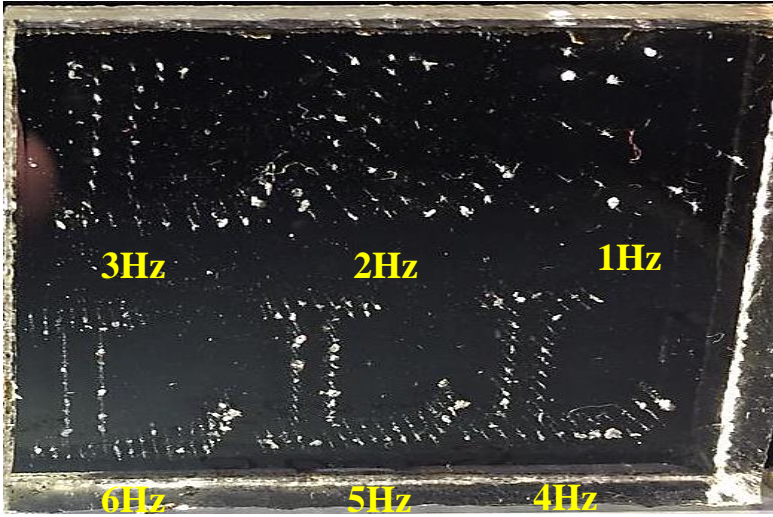
Figure 3.15 pulse repetition rate changing effect in dots per unit area in PMMA at energy a.360 mJ b.460 mJ   c.560 mJ.

3.3 Scanning electron microscope results

SEM images were captured to explore the morphology of the damaged zone inside BK7 and PMMA. Analysis of the SEM images is necessary to understand what is going on during the engraving process.

When a beam of laser focused inside the transparent materials, it's cause an internal visible marks. There are at least two different theories that explain how the subsurface marking mechanism works, the first one is that applying the right laser with appropriate energy density changes the refractive index of the material, which is a measure of how a light ray changes as it pass through a medium. The result is a visible mark.

The second explanation is that the laser delivers so much heat to a small area where a "micro-explosion" occurs. These micro-explosions create voids that are surrounded by denser areas, which change the light-scattering characteristics of the material and result in the mark.

From the BK7 SEM images in the Figures (3.16), (3.17), (3.18) different effects were noticed. From Figure (3.16 d) and Figure (3.17c) melting and resolidification of the BK7 was suggested. Very small spherical parts are found. There is a stress around the dot, as can be seen in Figure (3.16c), void has been detected from the Figure (3.18). From all these images, micro explosion inside the material with high temperature causing void, stresses, melting and resolidification was suggested.

From the images of PMMA figures (3.19) and (3.20), it is obvious there was degradation (vaporization) in the center of the dot and the region that surrounded the vaporization area is totally melted (softening) as it is shown in the figures mention above.
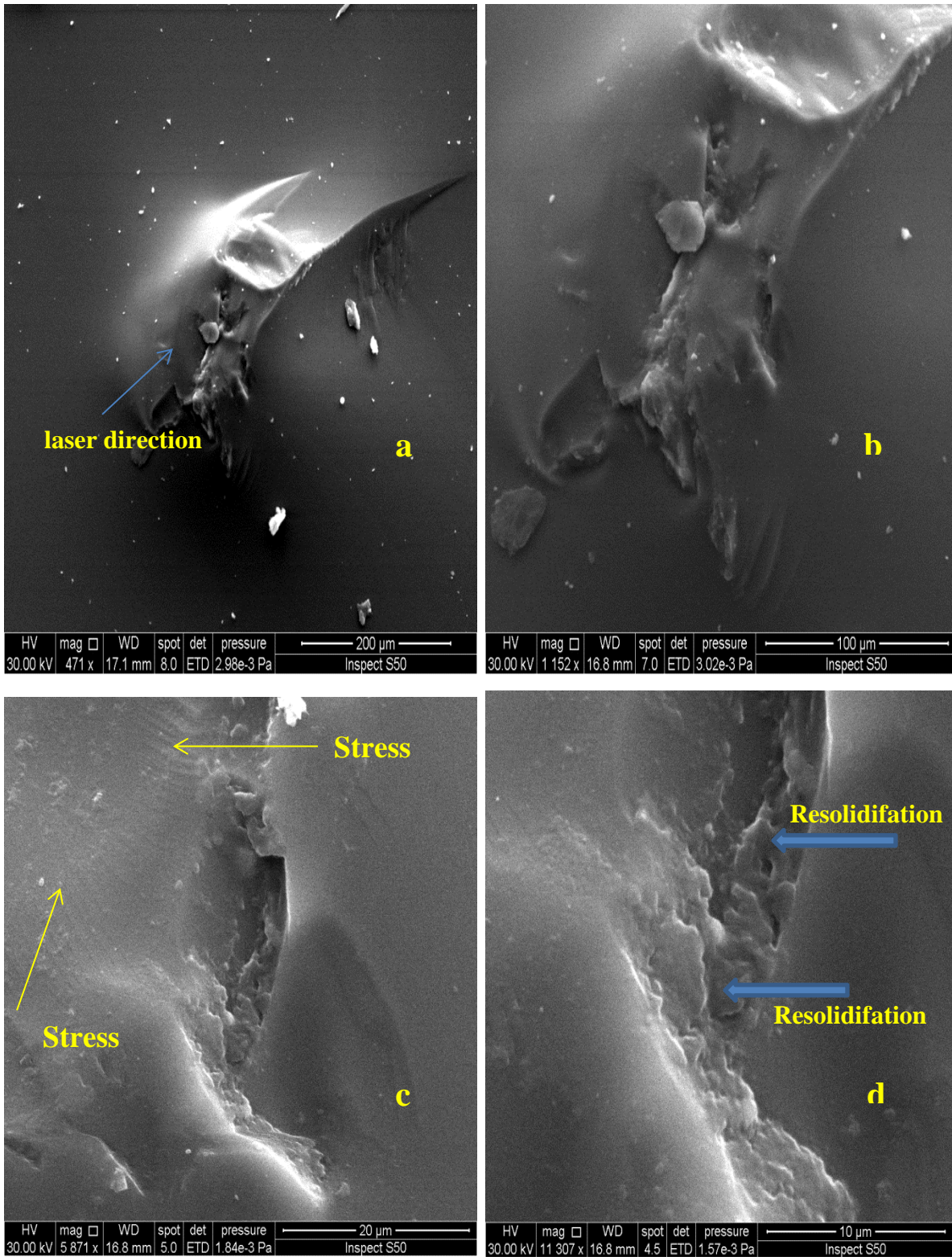
Figure 3.16 SEM side view images for damaged zone inside BK7glass at energy 900mJ and 1064 nm wavelength

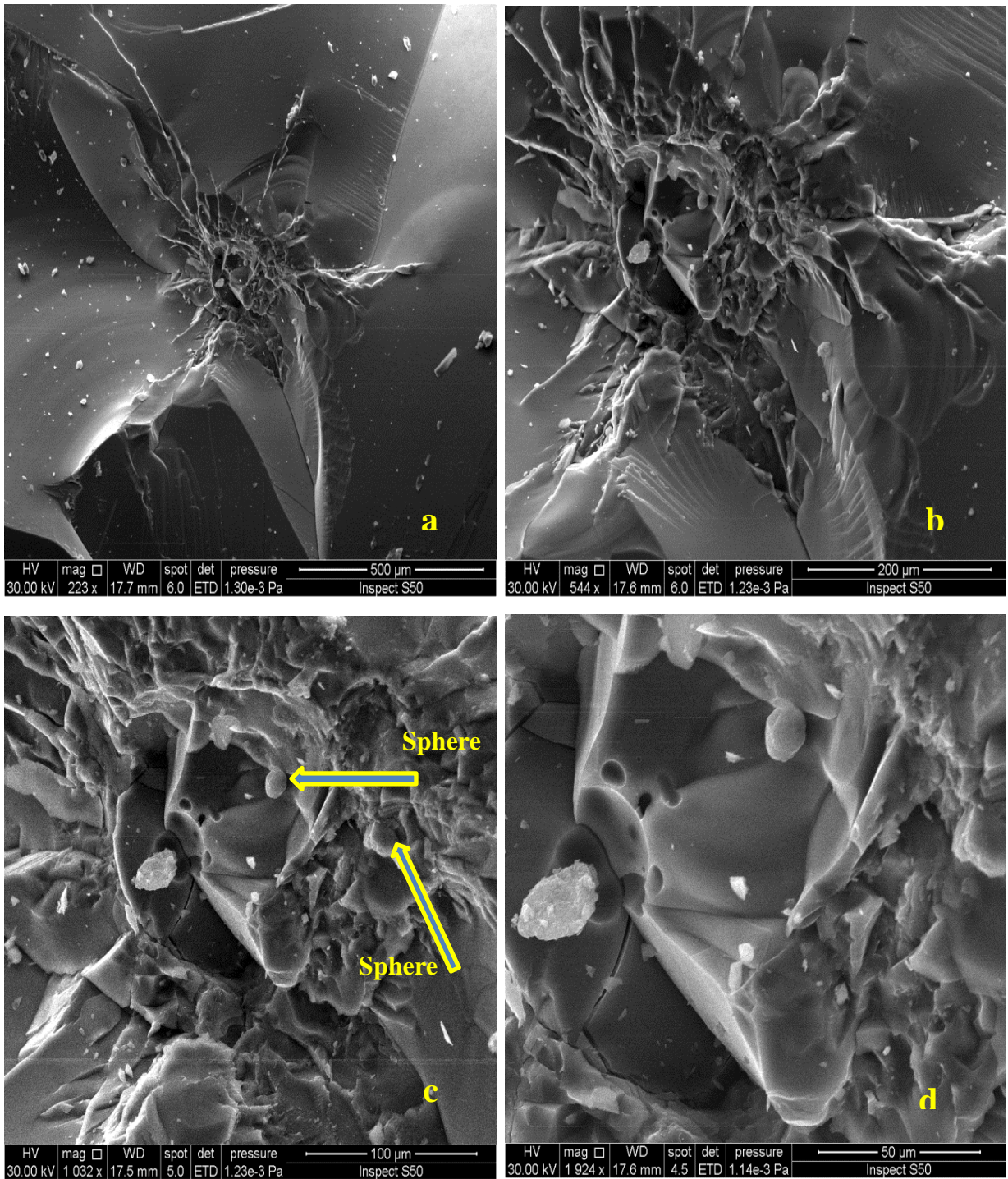**Figure 3.17** SEM images(top view) of dot in BK7 glass at energy 1000mJand 1064 nm wavelength
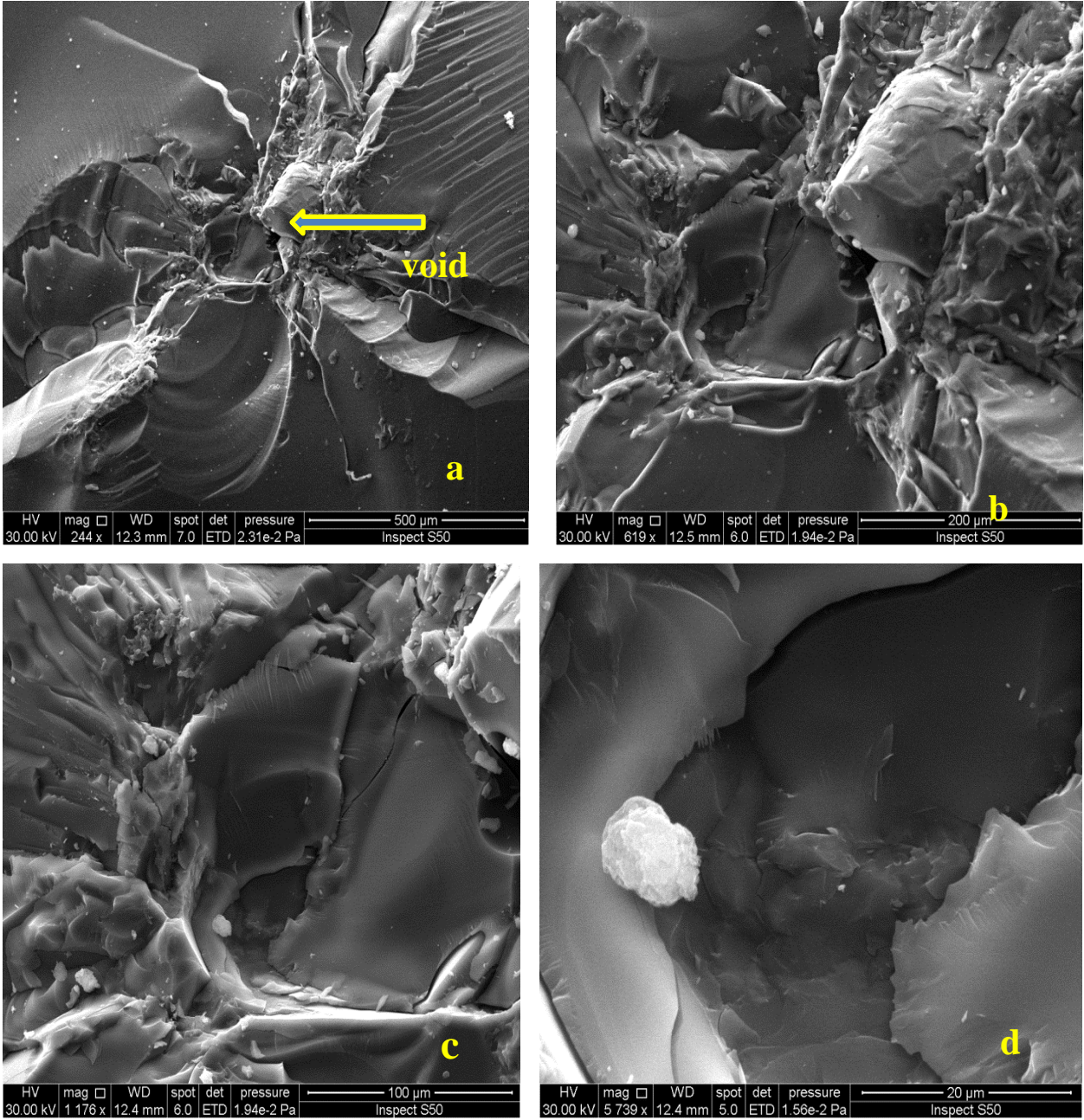
Figure 3.18 SEM images (top view) of BK7 glass at 900mJ energy and 1064nm wavelength
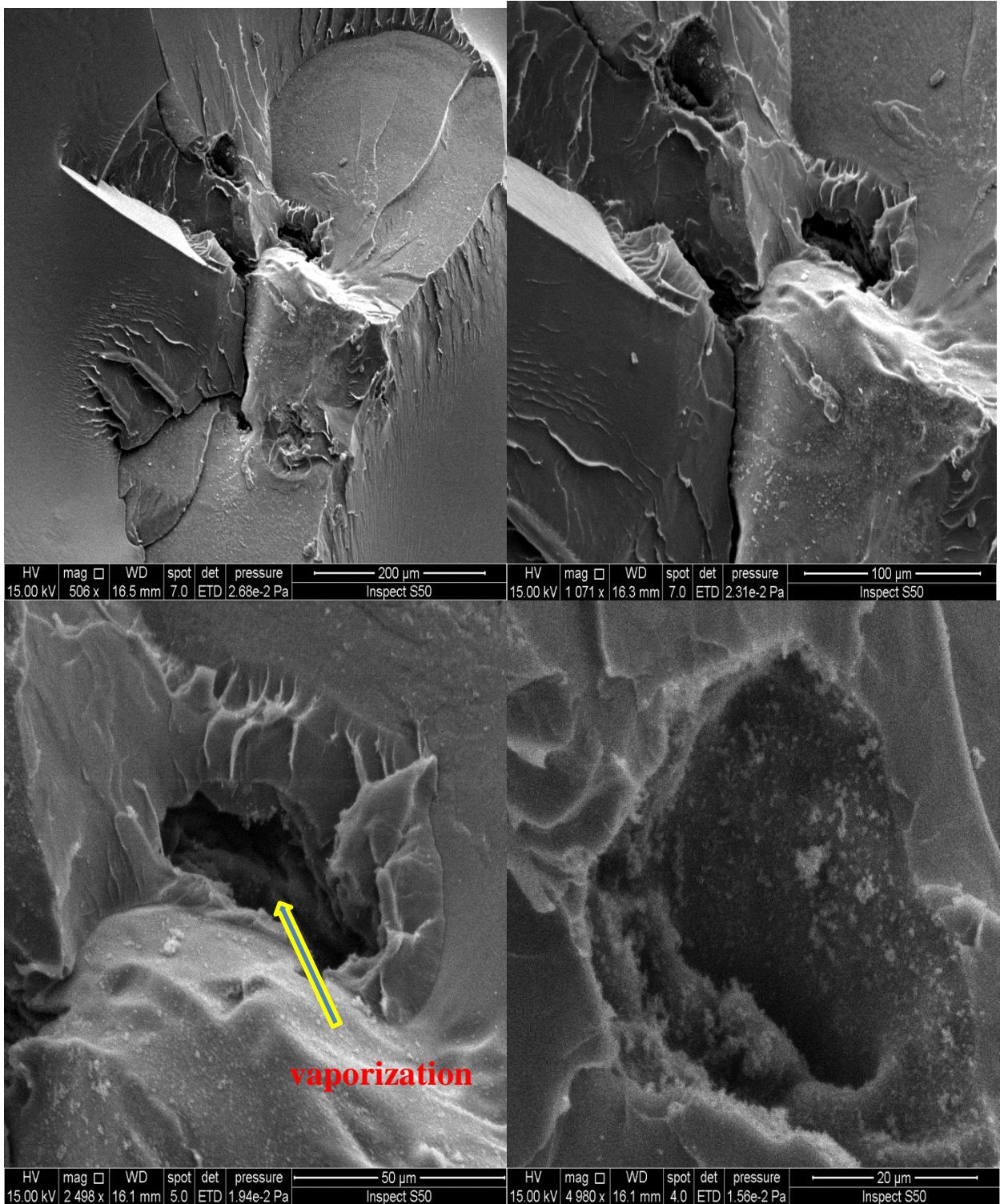
Figure 3.19 SEM images (top view) of PMMA at 600 mJ energy and 1064 nm wavelength
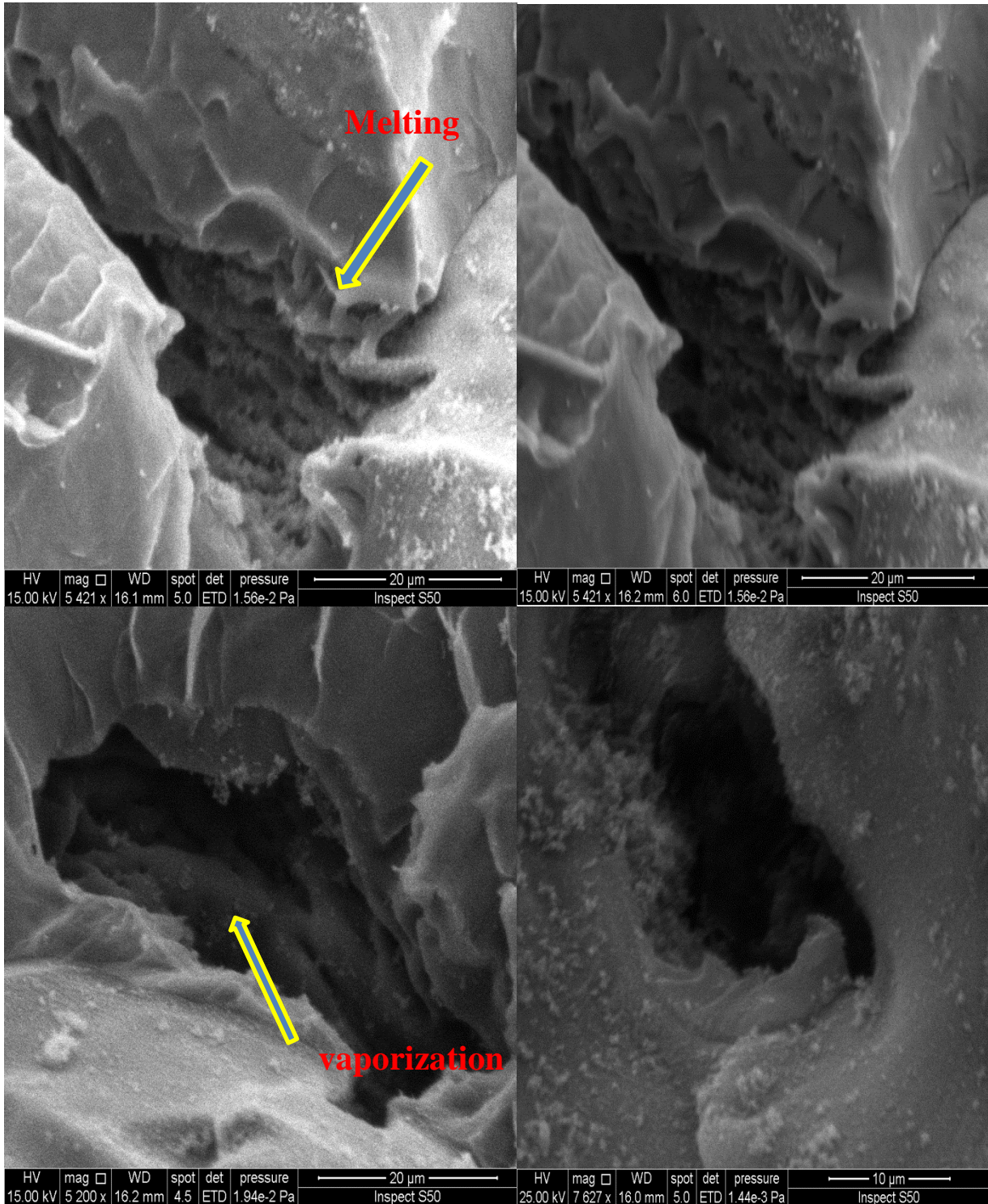
Figure 3.20 SEM images (top view) of PMMA at 600 mJ energy and 1064 nm wavelength

3.4 Computation results

The simulation part of this study has been achieved with different laser energies for BK7 to investigate the effect of changing the laser energy on the dots area and penetration depth by using the same conditions and parameter that were used in the experimental work, by using COMSOL Multiphysics V 4.3b.

The temperature distribution appears when the laser pulse hits the BK7 sample.

3.4.1 Laser power effect

The same Laser powers was applied in the experimental part will be also applied in the simulation and they were 0.1875MW, at 0.4375MW, 0.6875MW and 0.875MW,with wavelength 1064nm,pulse duration 4ns and spot size 100µm.

Figures (3.21), (3.22), (3.23) and (3.24) illustrate the temperature distribution in BK7 using single pulse technique. The maximum temperature was $917\,℃$ at the maximum power (0.875) MW and the minimum temperature was $615\,℃$ at the minimum power 0.1875 MW, and both of them are above the melting point.

Dots radius and depth could be measured from Figures (3.25), (3.26) (3.27)and(3.28) for laser power 0.1875MW, at 0.4375MW, 0.6875MW and 0.875MW respectively. The dots radius are measured at maximum temperature but the depth is measured at melting point which is equal to 557˚C. cross section view for every power is shown in Figures (3.29),(3.30),(3.31)and (3.32).
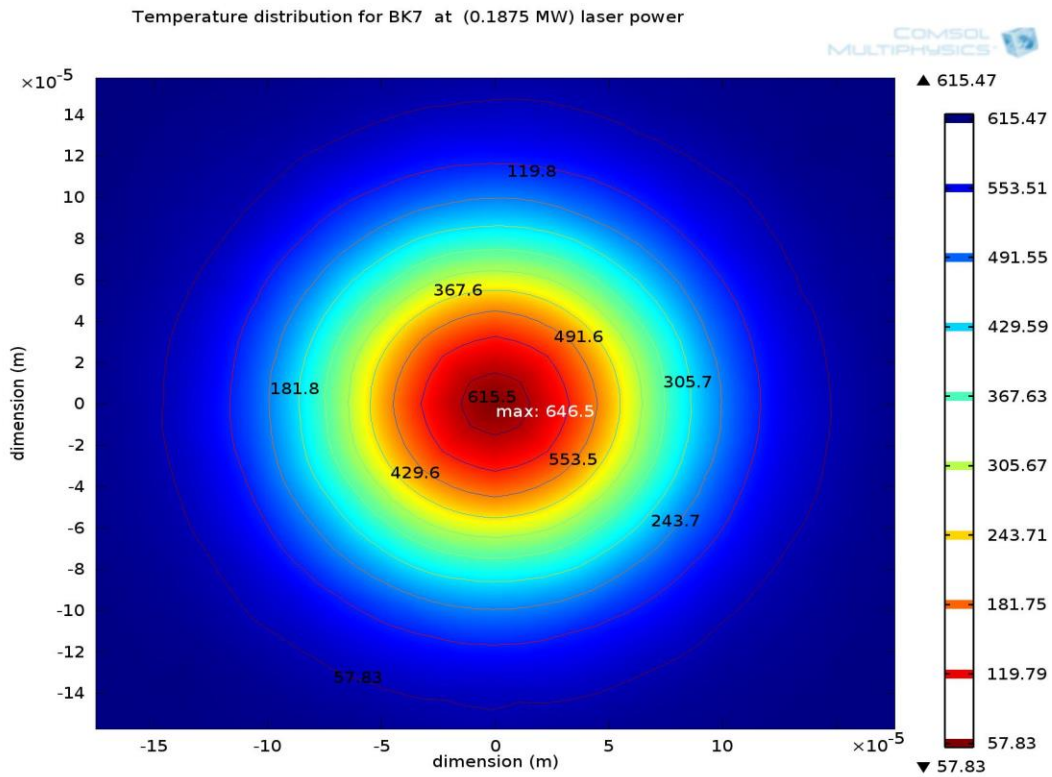
Figure 3.21 top view of the temperature distribution for BK7 at 0.1875MW laser power.
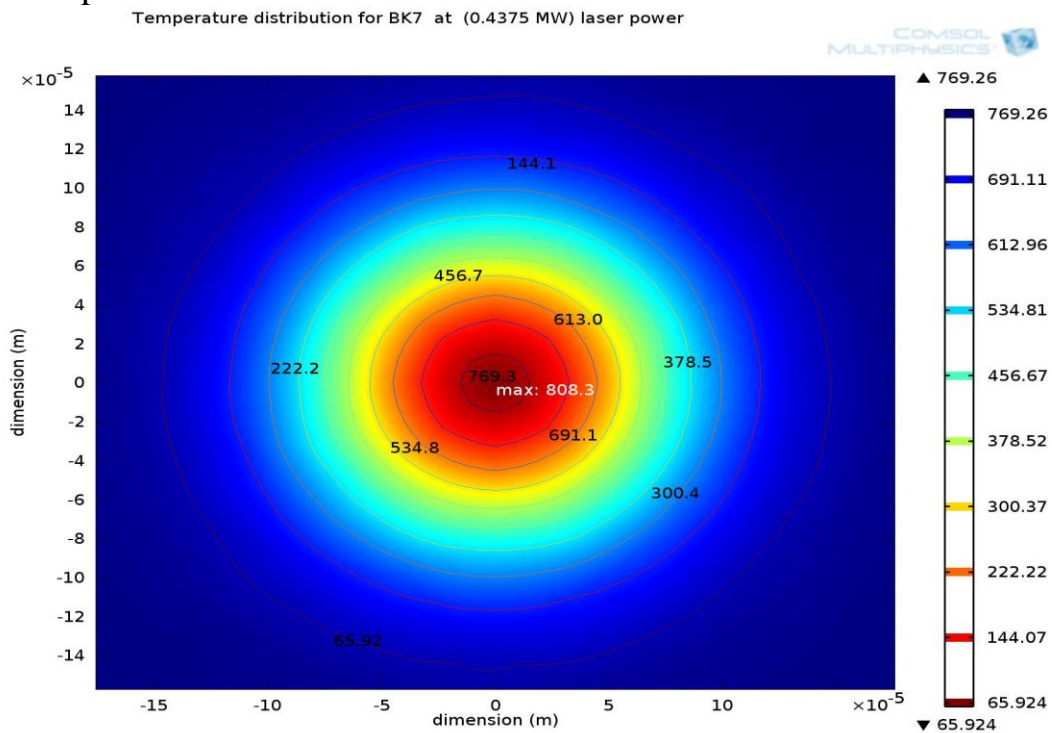
Figure 3.22 top view of the temperature distribution for BK7 at 0.4375MW laser power.
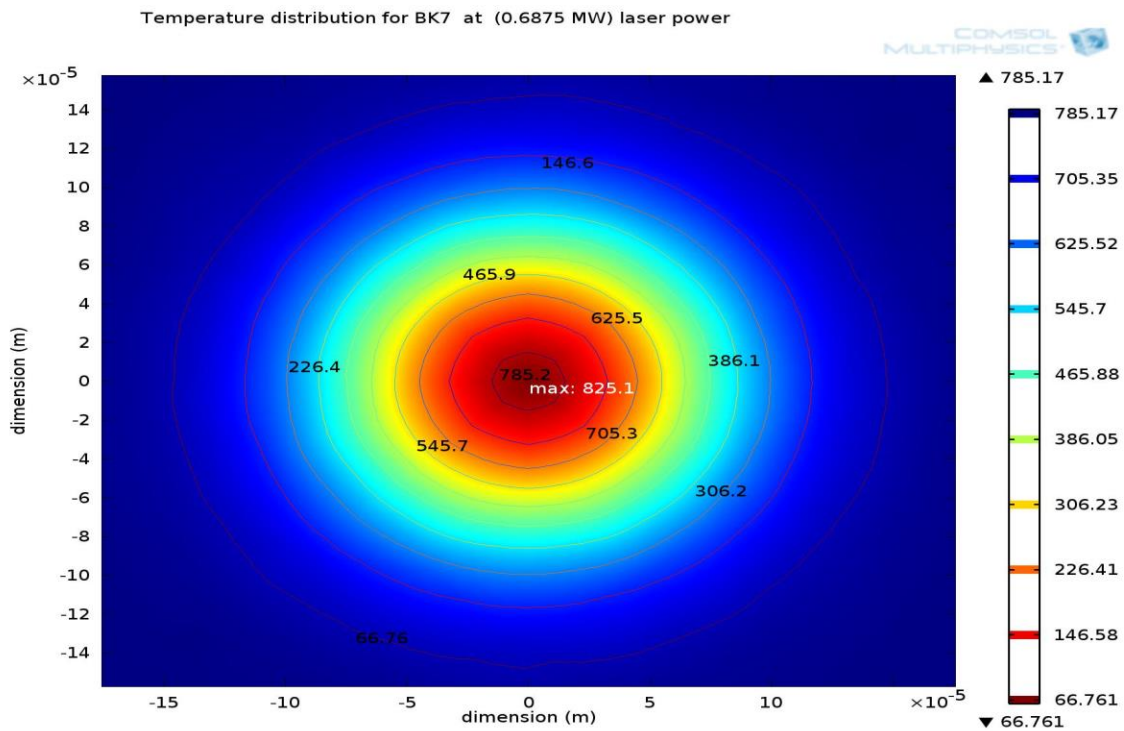
Figure 3.23 top view of the temperature distribution for BK7 at 0.6875MW laser power
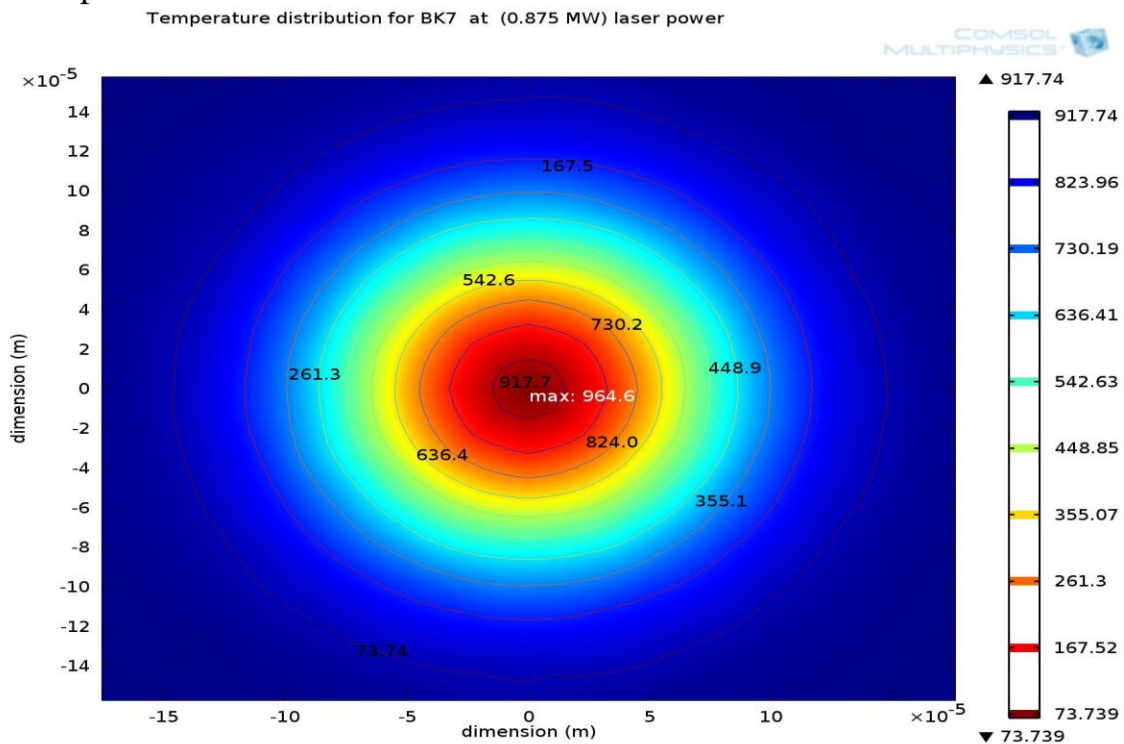
Figure 3.24 top view of temperature distribution for BK7 at 0.875MW laser power
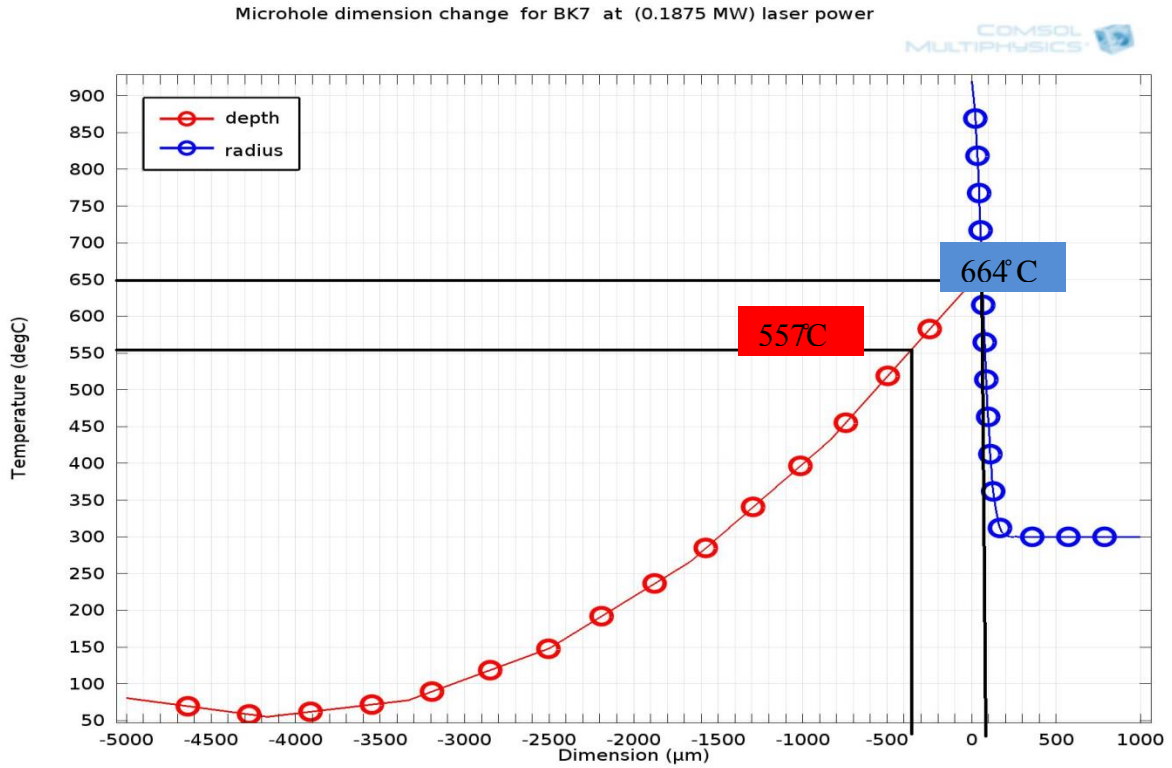
Figure 3.25 dot dimension at laser power (0.1875)MW
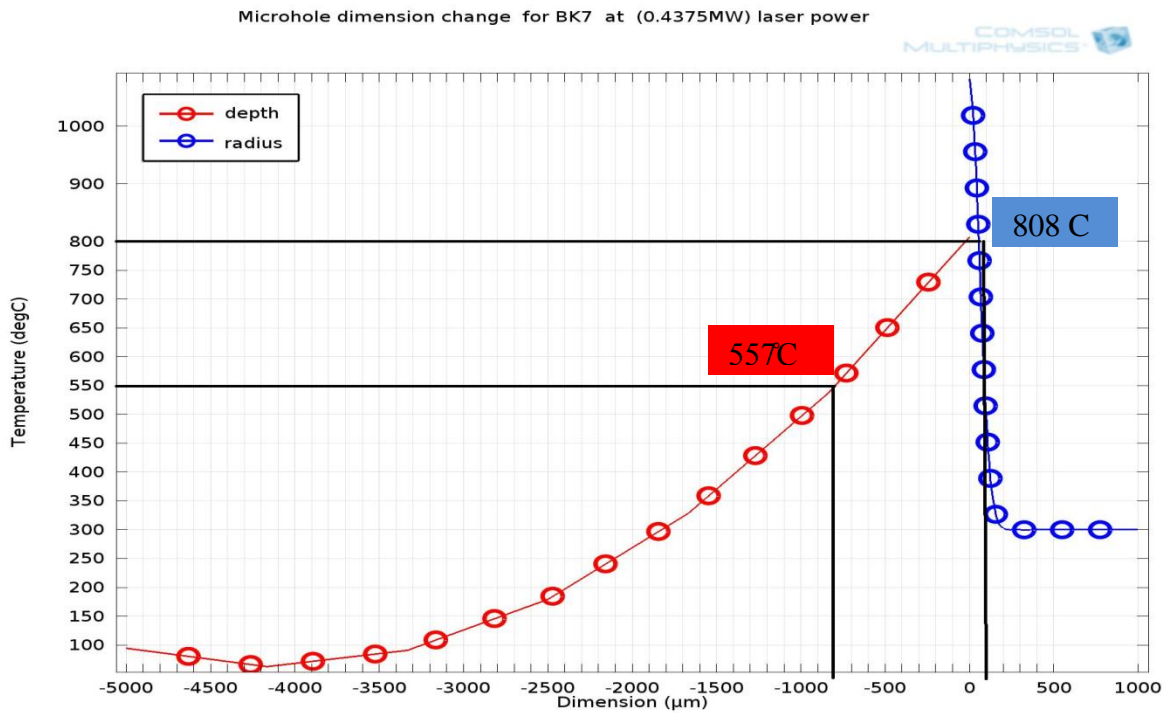
Figure 3.26 dot dimension at laser power (0.4375)MW
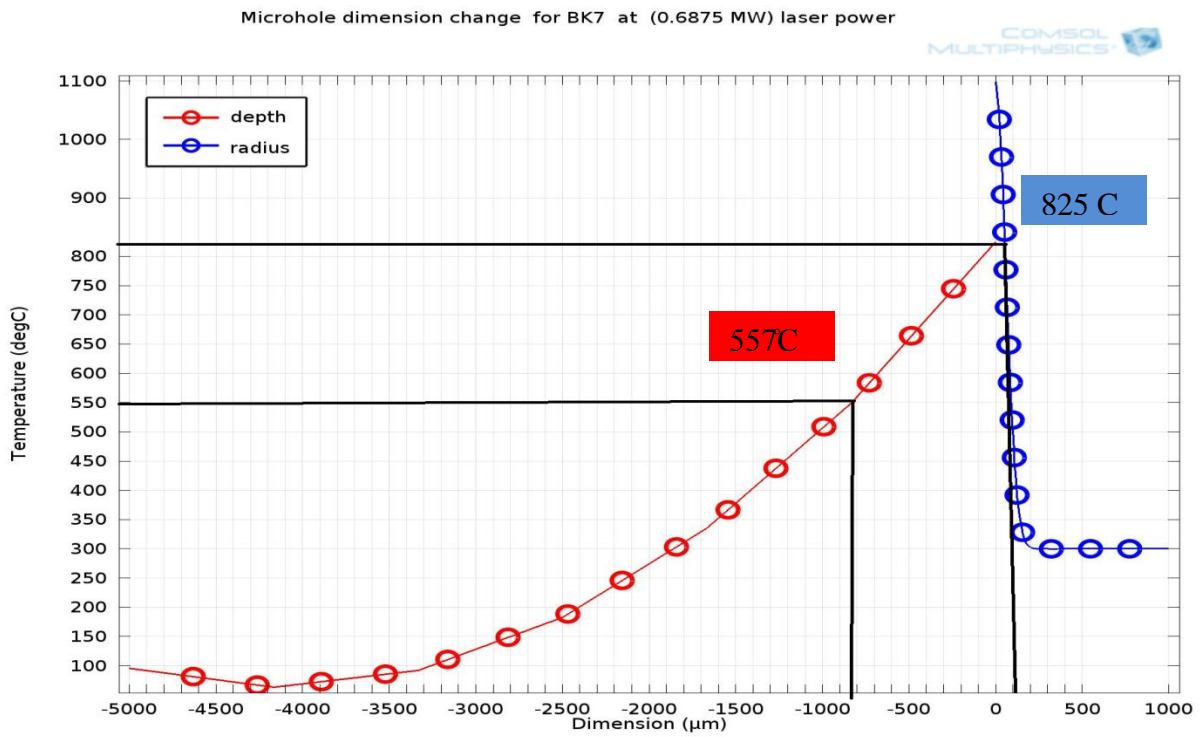
Figure 3.27 dot dimension at laser power (0.6875)MW
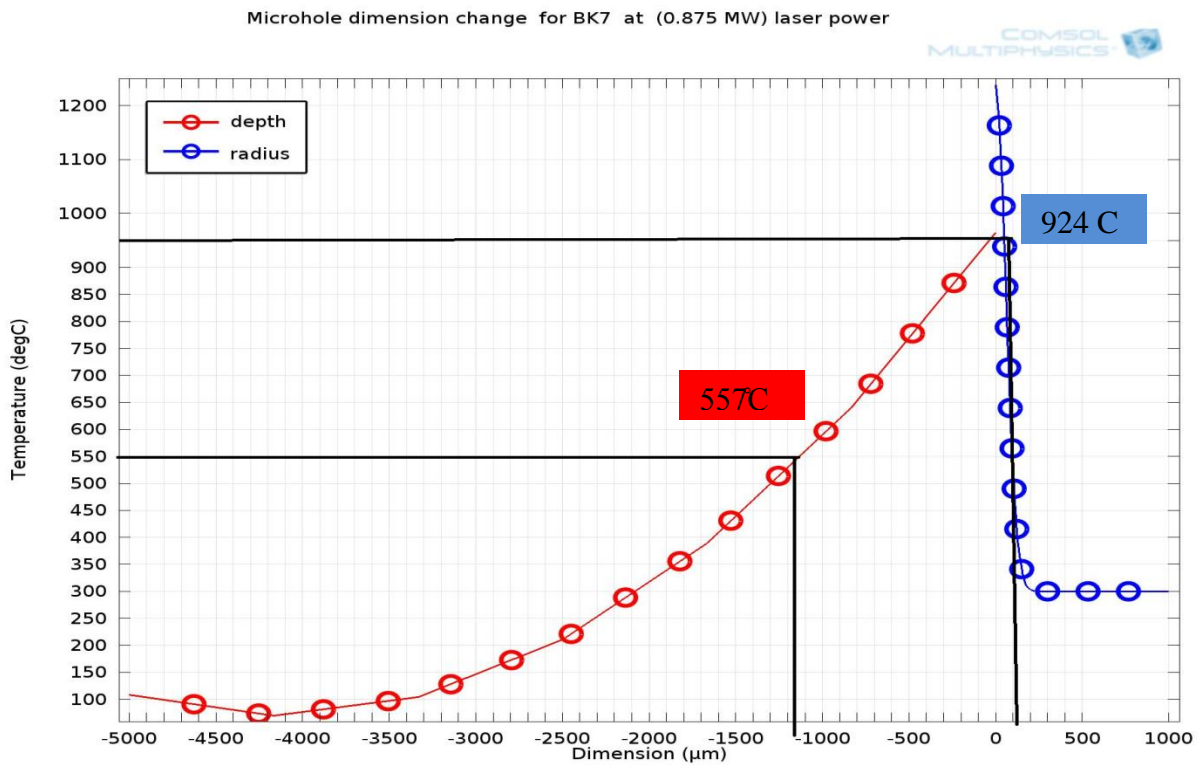
Figure 3.28 dot dimension at laser power (0. 875)MW

Figure 3.29 cross section view for BK7 glass at (0.1875)MW
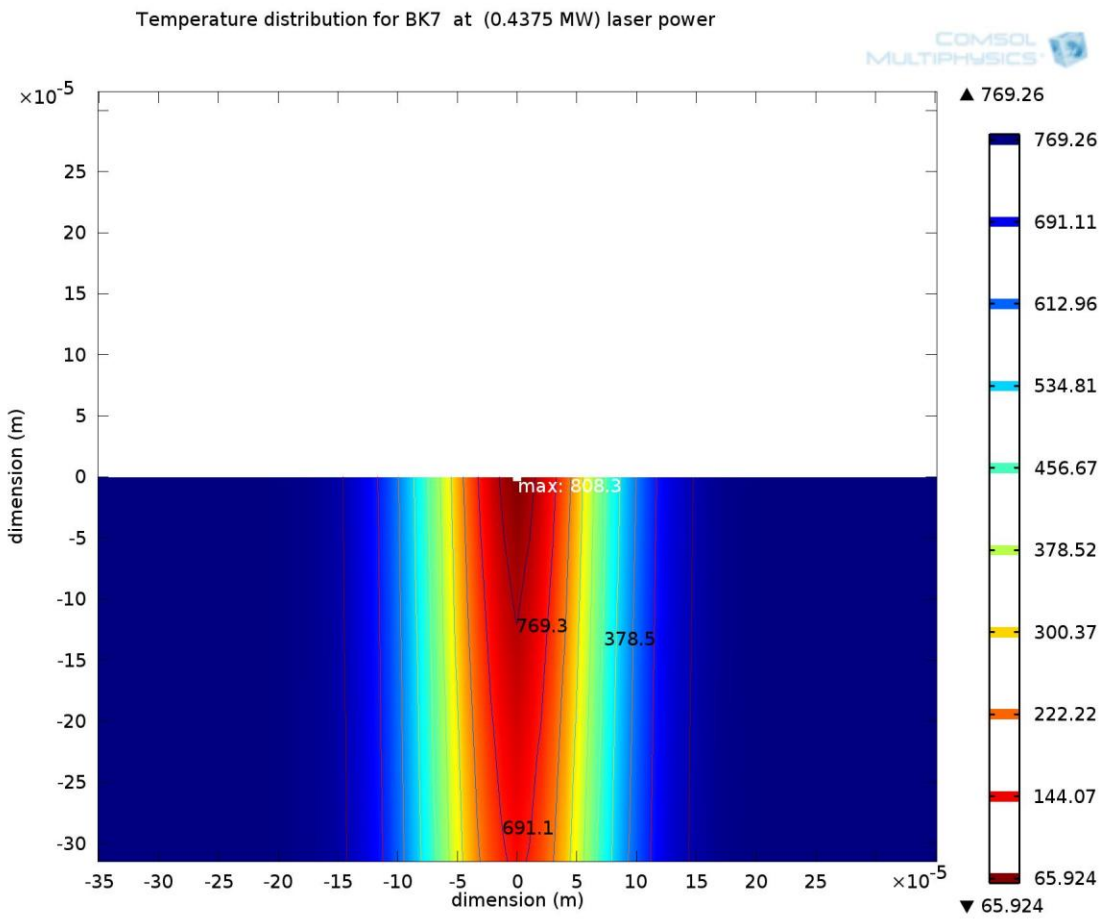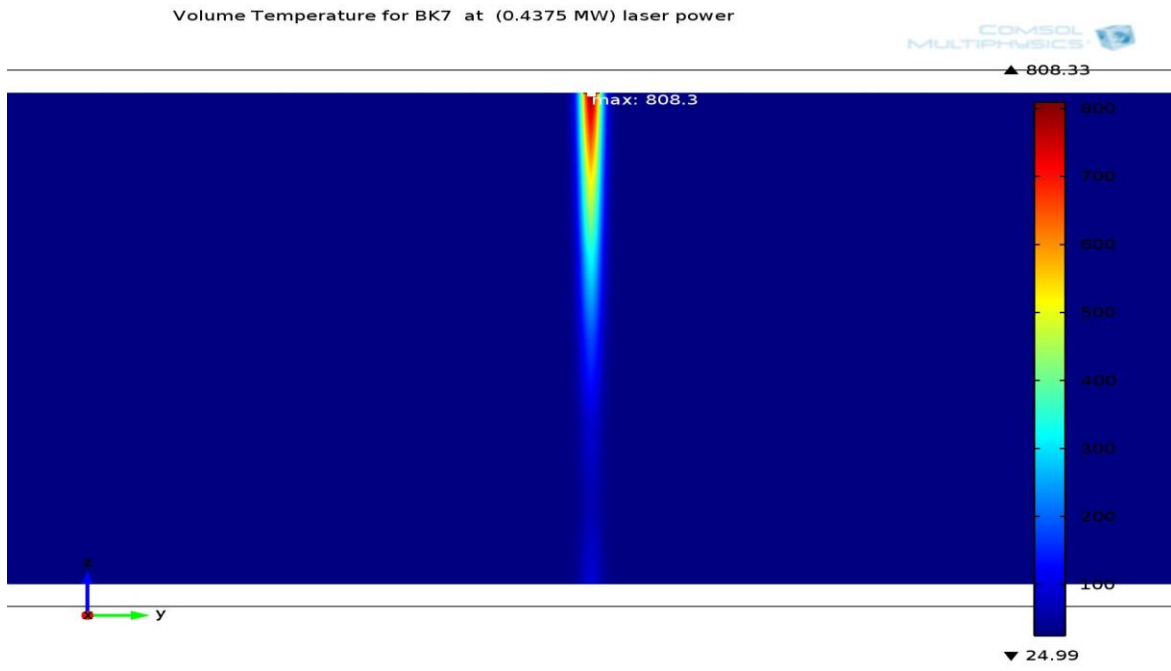
Figure 3.30 cross section view for BK7 glass at (0.4375)MW

Volume Temperature for BK7 at (0.6875 MW) laser power
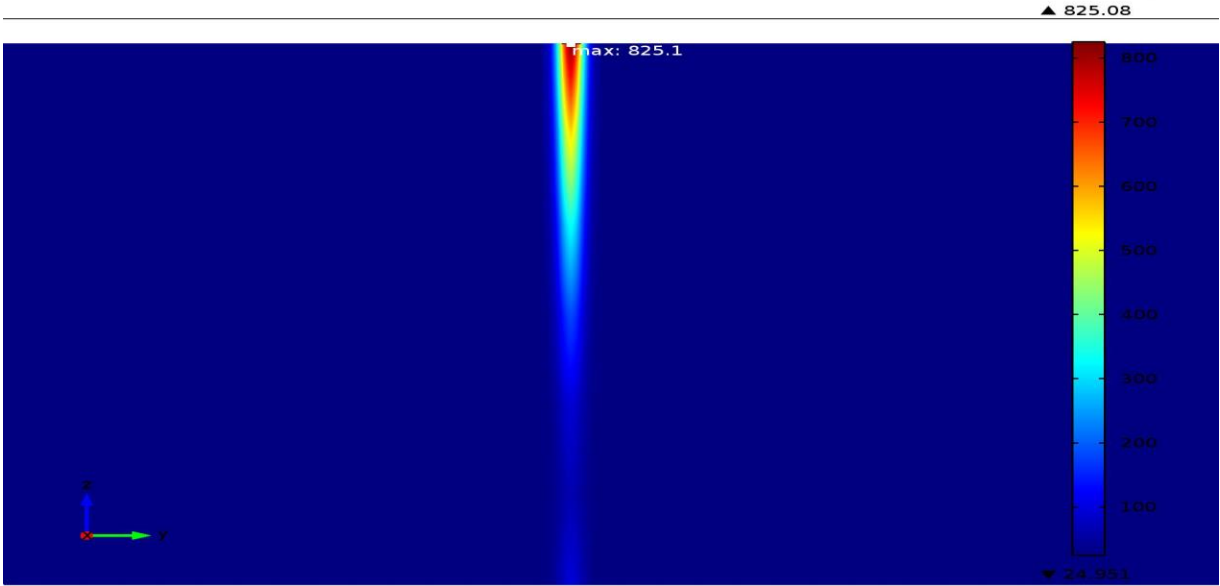
Temperature distribution for BK7 at (0.6875 MW) laser power
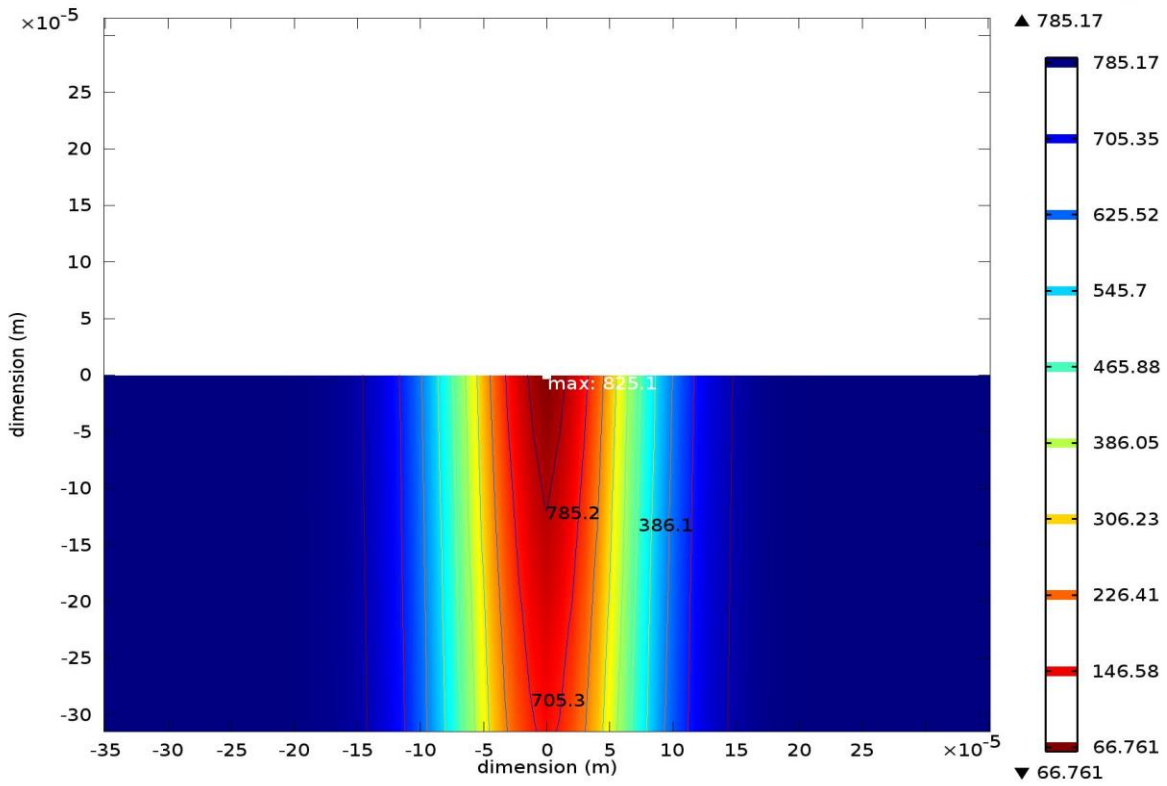
Figure 3.31 cross section view for BK7 glass at(0.6875)MW

Volume Temperature for BK7 at (0.875 MW) laser power

▲ 964.63

max: 964.6

Temperature distribution for BK7 at (0.875 MW) laser power

▲ 917.74

	917.74
	823.96
	730.19
	636.41
	542.63
	448.85
	355.07
	261.3
	167.52
	73.739

max: 964.6

917.7   448.9

824.0

▼ 73.739
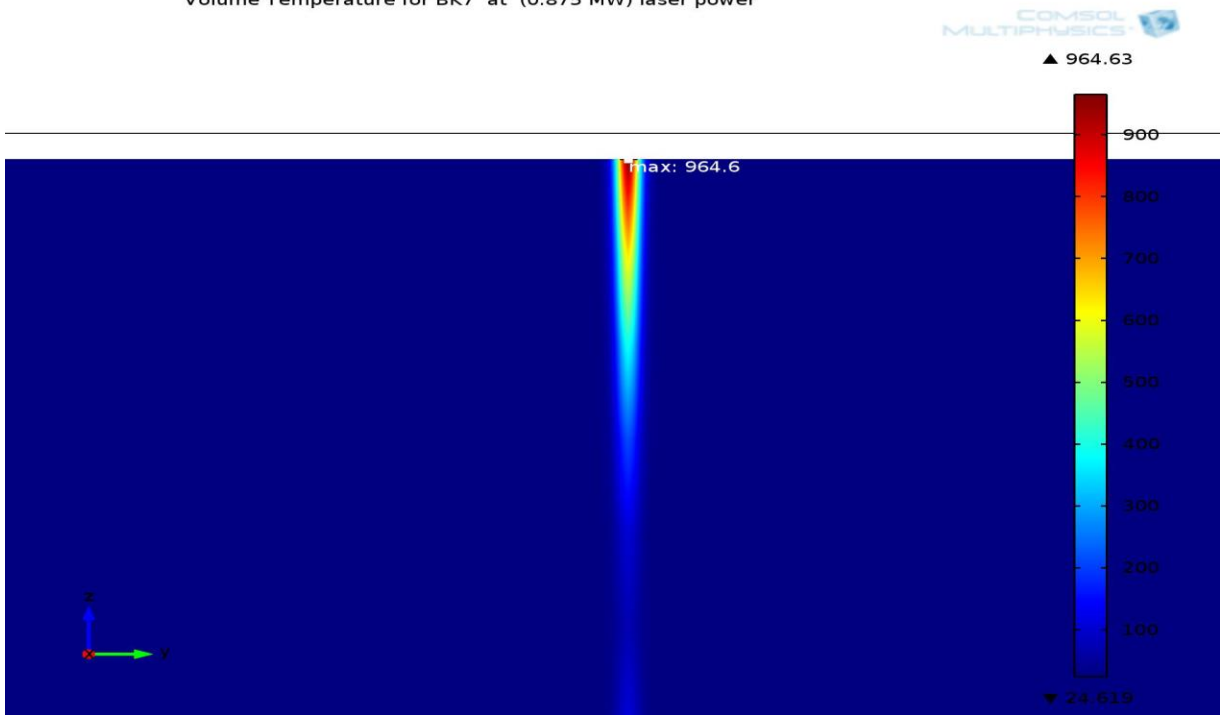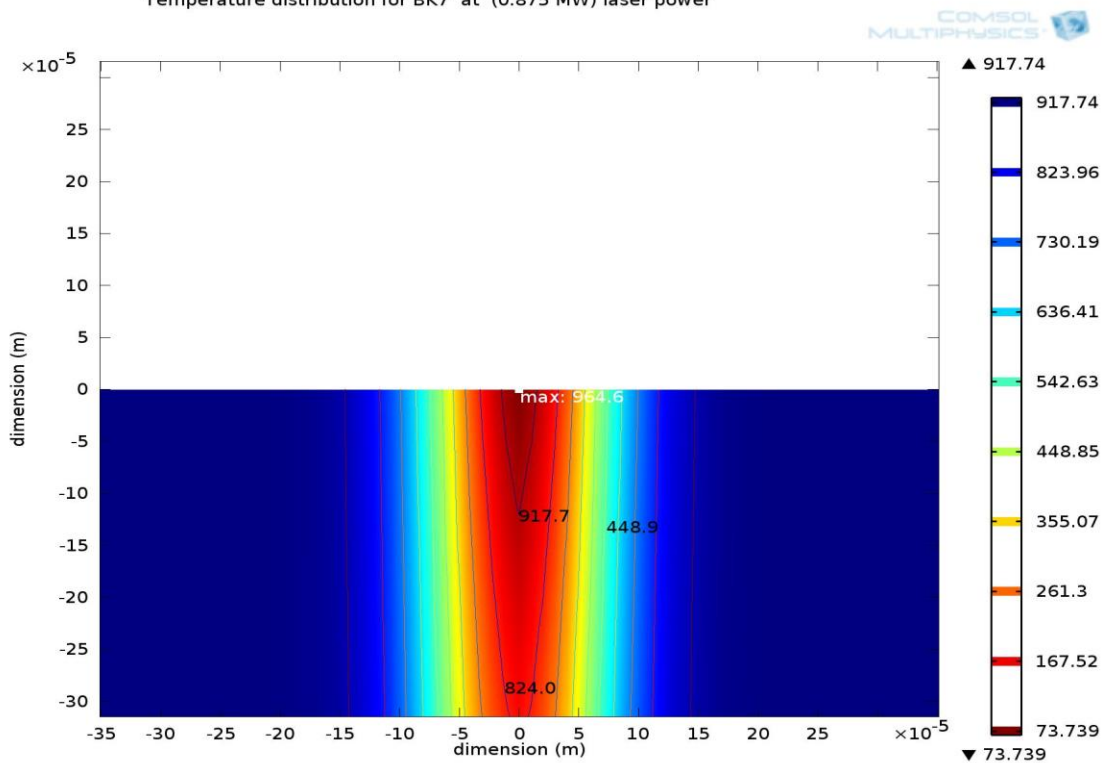
Figure 3.32 cross section view for BK7 glass at (0. 875)MW

3.4.2 Comparison between theoretical and experimental results

The results of the experimental part listed earlier in this chapter, are compared with the simulation results in the same rang of power. Figure (3.33) shows is for the radius results while Figure (3.34)shows the depth results.
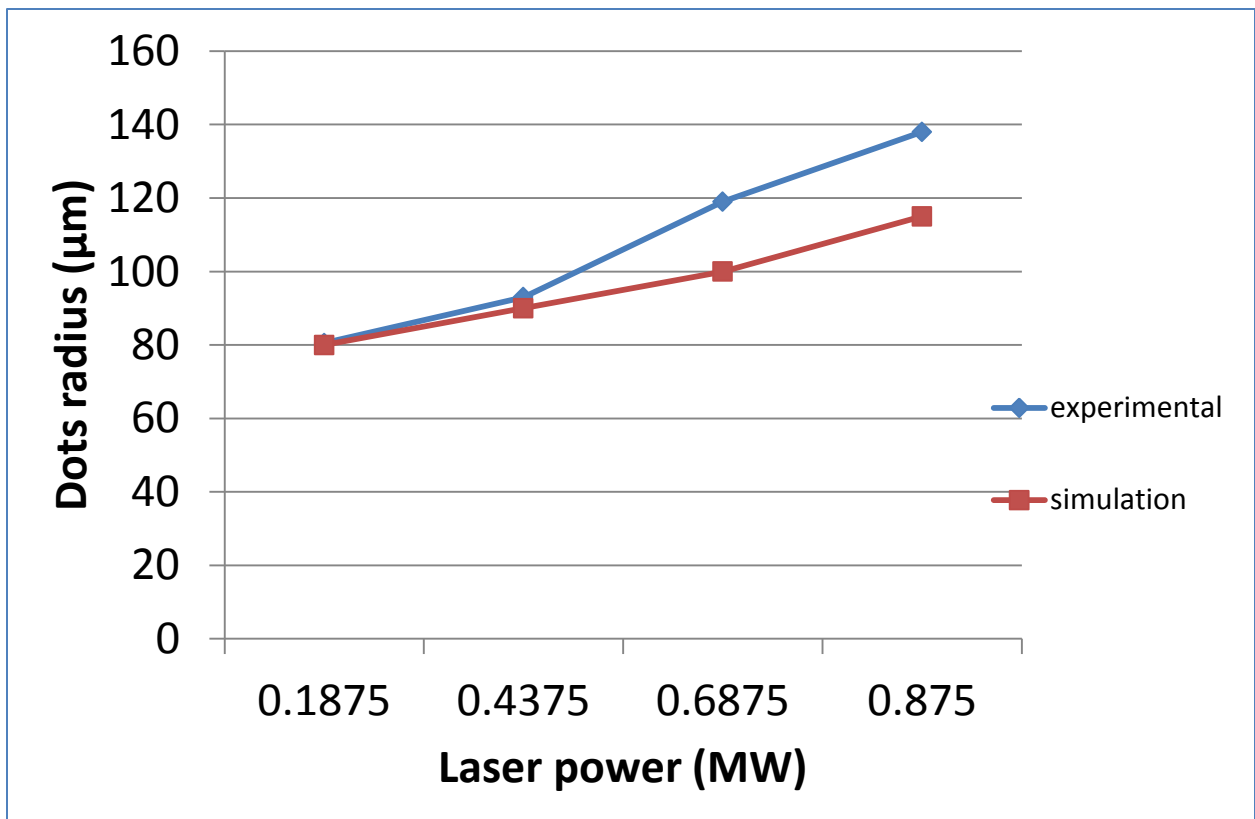
Figure 3.33 Comparison of dots radius differences between experimental and simulation
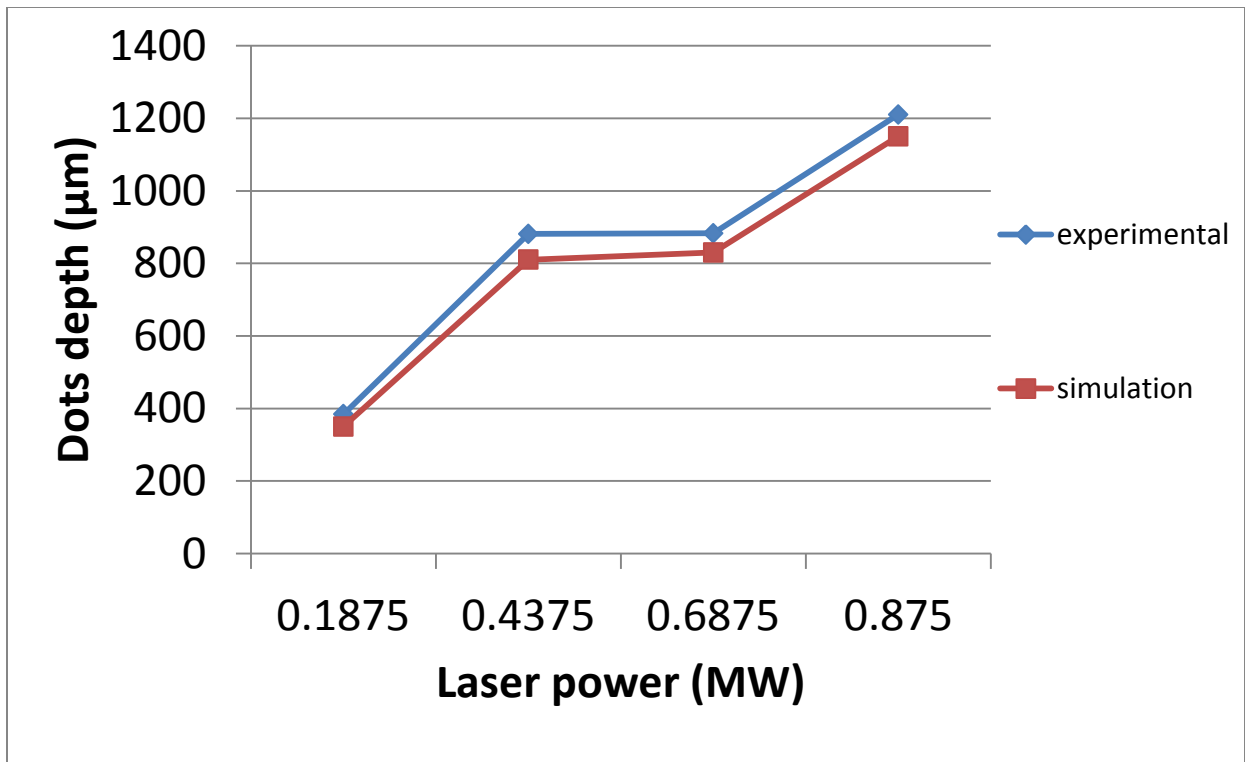
Figure 3.34 Comparison of dots depth differences between experimental and simulation

There are differences in the dot depth and radius between the experiment and the simulation .The percentage of differences is 10% to 15% for BK7. That is why the simulation gives reasonable results and good indication for the temperature distribution inside the material.

All the power used produce temperature above the melting point of BK7.

The Simulation results showed a good matching with the experimental one.

From all the previous experiments, results can be summarized as; Laser energy is a very important parameter in this application, it is capable of changing dots area and shape for both BK7 and PMMA. Under the microscope the PMMA dots compared with BK7 dots are associated with less cracks and well-formed damage are , but with naked eye BK7 dots appear to have more clarity, dots that are induced with 1064nm wavelength are larger in area than those induced with 532nm wavelength for both PMMA and BK7.

For a achieving the best dots in term of dots area and penetration depth , one pulse should be applied at the same site because increasing the number of pulses at the same site induce material distortion and overlapping with adjacent dots which is lead to failure of the material.

The dots also affected by the focal position, nearest focal position to the surface will induce dot with larger area than deeper focal position, this attribute to losses in laser energy.

Feed rate of the CNC work station has important role in the sub surface laser engraving application, feed rate combined with pulse repetition rate and laser energy are responsible for the image resolution.

The suggested mechanism that explains this damage is due to micro explosion that occurs inside the material causing void and material shattering.

3.5 Conclusions

Sub surface laser engraving for BK7 and PMMA has been achieved by using Nd:YAG laser with two wavelengths 532nm and 1064 nm, many parameters have been examined to recognize its effect on the final results such as laser energy ,laser wavelength, focal position effect ,feed rate ,pulse repetition rate and number of pulses, from all these parameters the results show :

1. Increasing laser energy leads to increase the dots area and expand the surrounding cracks in BK7 and PMMA.

2. At the same laser energy, dots area in PMMA are larger than in BK7 due to the difference in melting point of BK7 and PMMA and the surrounding cracks in BK7 is more than in PMMA.

3. Laser focal position has remarkable effect on the dots area, which decrease as the focal plane position becomes deeper inside the material specially in PMMA that attributed to the loss of energy and material inhomogeneity.

4. In BK7, laser wavelength has a significant effect on the dots area and the damage zone morphology, 532 nm produces dots with smaller area and more uniform than dots compared 1064nm.

5. Increasing the number of pulses at same place will expand the dots area and the penetration depth, more than 3 pulses will result in distortion of the dots shape

6. Decreasing the feed rate leads to improve the resolution due to the increase in number of dots per unit area but with limits because very slow feed rate produce distorted model.

7. Micro Explosion has been occurred inside the material, forces the material fragments away from center which will cause a void and material melting and resolidification.

8. For this application, BK7 is more convenient than PMMA, but PMMA still promising alternative choice.

9. Simulation results had a close match to the experimental results; the dimensions of the dimeter and the penetration depth were nearly the same.

3.6 Future work

The following are suggestions for the future work:

1. Examining another wavelength for nanosecond Nd-YAG, as in example, the third harmonic 335 nm.

2. Studying the effect of pre-heating the workpiece before laser shooting, the dots area and shape.

3. Employing laser with shorter pulse duration (femtosecond laser) with different spot size and studying its effect on the results.

4. Varying the laser incident angle on the sample and finding out the difference in shape in every angle.

References

[1]   Kochergin, S.A., Morgunov, Y.A. and Saushkin, B.P., Surface Manufacturing Under Pulse Fiber Laser. Procedia CIRP, 42, (2016).

[2]   Ion, J.,. Laser processing of engineering materials: principles, procedure and industrial application. Butterworth-Heinemann. (2005).

[3]   Maini, A.K., Lasers and optoelectronics: fundamentals, devices and applications. John Wiley & Sons (2013).

[4]   Diels, J.C. and Arissian, L. Lasers: the power and precision of light. John Wiley & Sons (2011).

[5]   Lenk, A. and Witke, T.,. Decoration of Glass by Surface and Sub-surface Laser Engraving. In Optics and Lasers in Biomedicine and Culture. Springer Berlin Heidelberg. pp. 155-158 (2000).

[6]   Verburg, P.C., Laser-induced subsurface modification of silicon wafers (Doctoral dissertation, University of Twente) (2015).

[7]   Buchroithner, M. ed., True-3D in cartography: autostereoscopic and solid visualisation of geodata. Springer Science & Business Media (2012).

[8]   Honma, T., Benino, Y., Fujiwara, T. and Komatsu, T.,. Line patterning with large refractive index changes in the deep inside of glass by nanosecond pulsed YAG laser irradiation. Solid state communicationspp.193-196 (2005).

[9]   Gattass, R.R. and Mazur, E., Femtosecond laser micromachining in transparent materials. Nature photonics, 2(4), pp.219-225 (2008).

[10]   Ganeev, R.A.,. Laser-surface interactions. Springer Science & Business Media (2013).

[11]   Dutta Majumdar, J. and Manna, I. Laser material processing. International materials reviews, 56(5-6), pp.341-388 (2011).

[12]   Dahotre, N.B. and Harimkar, S. Laser fabrication and machining of materials. Springer Science & Business Media (2008).

[13] Sugioka, Koji, Michel Meunier, and Alberto Piqué. Laser precision microfabrication. Springer (2010).

[14] William, M. Steen, and Mazumder Jyotirmoy. "Laser material processing." Steen springer-Verlag, London, Berlin, Heidelberg 3: 408 (2010).

[15] Dong, Liang, and Bryce Samson. Fiber Lasers: Basics, Technology, and Applications. CRC Press (2017).

[16] Hashmi, Saleem. Comprehensive materials processing. Newnes (2014).

[17] Hallo, Ludovic, et al. "Laser-matter interaction in transparent materials: confined micro-explosion and jet formation." Extreme Photonics & Applications. Springer Netherlands (2010).

[18] Sugioka, Koji, and Ya Cheng. "Femtosecond laser processing for optofluidic fabrication." Lab on a Chip (2012).

[19] Tan, Deyao, ed. Engineering Technology, Engineering Education and Engineering Management: Proceedings of the 2014 International Conference on Engineering Technology, Engineering Education and Engineering Management (ETEEEM 2014), Hong Kong, 15-16 November 2014. Crc Press, (2015).

[20] Donges, Axel, and Reinhard Noll. Laser Measurement Technology: Fundamentals and Applications. Vol. 188. Springer, (2015).

[21] Kannatey-Asibu Jr, Elijah. Principles of laser materials processing. Vol. 4. John Wiley & Sons, (2009).

[22] Schaffer, Chris B., Andre Brodeur, and Eric Mazur. "Laser-induced breakdown and damage in bulk transparent materials induced by tightly focused femtosecond laser pulses." Measurement Science and Technology(2001).

[23] Guo, Hengchang, et al. "The pulse duration dependence of femtosecond laser induced refractive index modulation in fused silica." Journal of Optics A: Pure and Applied Optics 6.8 (2004).

[24] Yu, Jingxia, et al. "Laser-induced damage initiation and growth of optical materials." Advances in Condensed Matter Physics (2014).

[25] Manenkov, Alexander A. "Fundamental mechanisms of laser-induced damage in optical materials: today's state of understanding and problems." Optical Engineering 53.1 (2014).

[26] Kuzuu, Nobu, et al. "Laser-induced bulk damage in various types of vitreous silica at 1064, 532, 355, and 266 nm: evidence of different damage mechanisms between 266-nm and longer wavelengths." Applied optics 38.12 (1999).

[27] Glezer, E. N., et al. "Three-dimensional optical storage inside transparent materials." Optics Letters 21.24 (1996).

[28] Bosman, Johan. Processes and strategies for solid state Q-switch laser marking of polymers. University of Twente, (2007).

[29] Sugioka, Koji, and Ya Cheng. Femtosecond laser 3D micromachining for microfluidic and optofluidic applications. Springer Science & Business Media(2013).

[30] Grigoropoulos, Costas P. Transport in laser microfabrication: fundamentals and applications. Cambridge University Press (2009).

[31] Shelby, James E. Introduction to glass science and technology. Royal Society of Chemistry (2005).

[32] Askeland, Donald R., and Pradeep Prabhakar Phulé. "The science and engineering of materials." (2003):

[33] Pfaender, Heinz G., ed. Schott guide to glass. Springer Science & Business Media, (1996)

[34] Vainos, Nikolaos A., ed. Laser growth and processing of photonic devices. Elsevier, (2012).

[35] Stoian, Razvan, et al. "Investigation and control of ultrafast laser-induced isotropic and anisotropic nanoscale-modulated index patterns in bulk fused silica." Optical Materials Express 3.10 (2013).

[36] Saldivar-Guerra, Enrique, and Eduardo Vivaldo-Lima. Handbook of polymer synthesis, characterization, and processing. John Wiley & Sons, (2013).

[37] Young, Robert Joseph, and Peter A. Lovell. Introduction to polymers. Vol. 2. London: Chapman & Hall, (1991).

[38] Gooch, Jan W. Polyimide Fiber. Springer New York, (2011).

[39] Miller, David C., et al. "Analysis of transmitted optical spectrum enabling accelerated testing of CPV designs." SPIE Solar Energy+ Technology. International Society for Optics and Photonics, (2009).

[40] Mottay, Eric, et al. "Industrial ultrafast internal engraving laser system for anti-counterfeiting applications." Lasers and Applications in Science and Engineering. International Society for Optics and Photonics (2008).

[41] Yilbas, Bekir Sami. Laser heating applications: analytical modelling. Elsevier, (2012).

[42] Yang, Steven T., et al. "Thermal transport in CO 2 laser irradiated fused silica: In situ measurements and analysis." Journal of Applied Physics 106.10 (2009).

[43] Lankalapalli, Kishore N., Jay F. Tu, and Mark Gartner. "A model for estimating penetration depth of laser welding processes." Journal of Physics D: Applied Physics 29.7 (1996).

[44] Stuart, B. C., et al. "Laser-induced damage in dielectrics with nanosecond to subpicosecond pulses." Physical review letters 74.12 (1995).

[45] Schaffer, Chris B., et al. "Micromachining bulk glass by use of femtosecond laser pulses with nanojoule energy." Optics letters 26.2 (2001).

[46] Du, Keming, and Peng Shi. "Subsurface precision machining of glass substrates by innovative." Glass Sci. Technol 76.2 (2003).

[47] Shin, Yongjin, et al. "Analysis of laser engraving image inside crystal and PMMA." Lasers and Applications in Science and Engineering. International Society for Optics and Photonics, (2005).

[48] Verburg, Paul Christiaan. Laser-induced subsurface modification of silicon wafers. Diss. Universiteit Twente, (2015).

[49] Guo-Hang, Hu, et al. "Wavelength dependence of laser-induced bulk damage morphology in KDP crystal: determination of the damage formation mechanism." Chinese Physics Letters 29.3 (2012).

Appendix A

Optical Glass (N-BK7 and B270 types)

APPLICATIONS: N-BK7 is a Schott™ designation for the most common Borosilicate Crown glass used for a wide variety of visible applications. The basic data here is given for N-BK7. Full optical design data on N-BK7 and other glasses can be found by following the web links at the bottom of this page.

Transmission Range	350nm to 2.5μm
Refractive Index	1.51680 @ 587.5618nm (Yellow Helium Line)
Reflection Loss	8.1% at 587.5618nm (2 surfaces)
Absorption Coefficient	--
Reststrahlen Peak	--
dn/dT	See Schott™ Table
dn/dμ = 0	--
Density	2.51
Melting Point	557°C (Transformation Temperature)
Thermal Conductivity	1.114 W m^{-1} K^{-1}
Thermal Expansion	7.1 x 10^{-6} K^{-1}
Hardness	Knoop 610
Specific Heat Capacity	858 J Kg^{-1} K^{-1}
Dielectric Constant	n/a
Youngs Modulus (E)	82 GPa
Shear Modulus (G)	n/a
Bulk Modulus (K)	34 GPa
Elastic Coefficients	n/a
Apparent Elastic Limit	63.5MPa (9206psi)
Poisson Ratio	0.206
Solubility	Insoluble in water
Molecular Weight	n/a
Class/Structure	Amorphous glass

WEBLINKS:
Schott Glass Catalogue - Data on all Schott™ Glass types here.

Optical Glass (N-BK7 and B270 types)

BK7 and B270 Optical Glass

BK7 and B270 Optical Glass
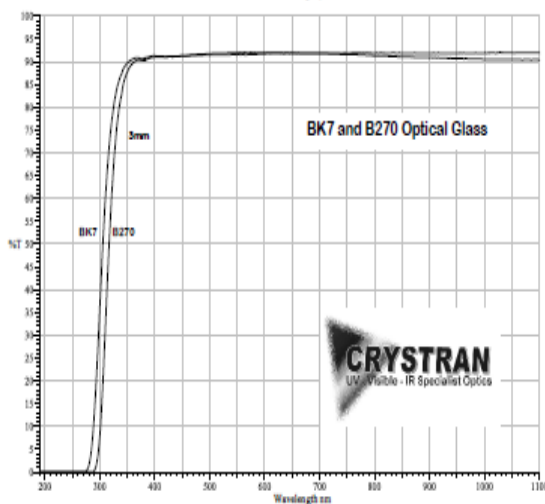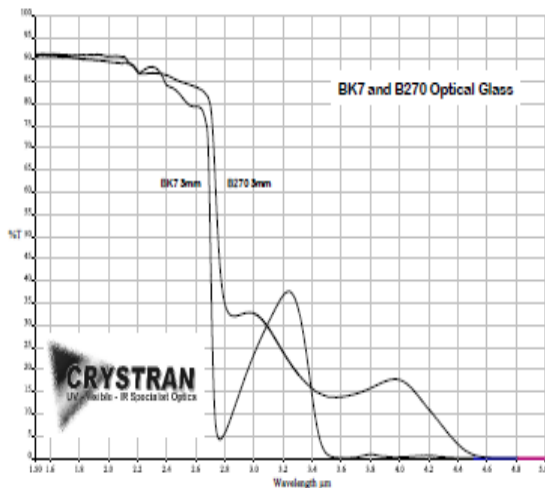
Appendix B

HSIN HWA CHEMICAL CO., LTD.

MATERIAL SAFETY DATA SHEET

1. CHEMICAL PRODUCT/ COMPANY DIENTIFICATION

PRODUCT NAME: CAST ACRYLIC SHEET

SUPPLIER : HSINHWA CHEMICAL CO., LTD. (TAIWAN)
NO.1 YUNG-HSIANG ROAD, FANG-LIAO HSIANG,
940, PINTUNG HSIEN, TAIWAN

Tel: 886-8-8667725   Fax: 886-8-8667732

2. PRODUCT COMPONENTS

COMPONENTS CAS REG. NO. WEIGHT (%)

1. Polymethyl methacrylate   (PMMA) 9010-88-2 99.5 (MIN)

2. Methyl methacrylate   (MMA) 80-62-6 0.5 (MAX)

3. PHYSICAL PROPERTIES

Appearance:	Clear to opaque solid
Odor:	N/A
Viscosity:	N/A
Melting Point:	150° C/300° F
Boiling Point:	N/A
Vapor Pressure:	N/A
Vapor Density:	N/A (Air =1)
Specific Gravity:	1.19 (Water =1)
pH:	N/A
Solubility in Water:	Negligible
Volatility:	Negligible (Weight %)
Evaporation Rate:	Negligible (Butyl Acetate = 1)

4. FIRE AND EXPLOSION HAZARD INFORMATION

Flash Point:	N/A
Auto Ignition Temperature:	445° C/833° F
Upper Explosion Limit (%):	N/A
Lower Explosion Limit (%):	N/A
Extinguishing Media:	Carbon dioxide, dry chemical, or water.
Fire Protection Equipment:	Wear self-contained, positive pressure breathing apparatus (MSHA/NIOSH approved, or equivalent) and full protective gear.
Unusual Fire and Explosion	Product is combustible thermoplastic material that burns vigorously

HSIN HWA CHEMICAL CO., LTD.

Hazard   with intense hea

5. WORKPLACE EXPOSURE LIMITS

COMPONENTS	OSHA		ACGIH	
	PEL	STEL	TLV	STEL
1. PMMA	None	None	None	None
2. MMA	100 ppm	None	100 ppm	None
3. Nuisance dusts (as particulates)	5 mg/m^3	None	10 mg/m^3	None

MMA: 100 ppm = 410 mg/ m^3

6. HAZARD INFORMATION

Hazard Scale:	0 = Insignificant, 1 = Slight, 2 = Moderate, 3 = High, 4 = Extreme
Health Designation:	1
Fire Designation:	1
Reactivity Designation:	0
Inhalation:	Inhalation of vapors from heated product can cause nausea, headache, dizziness as well as irritation of lungs, nose, and throat
Eye Contact:	Vapors from heated product can irritate the eye
Ingestion:	Low hazard associated with normal conditions
Skin Contact:	Possible skin irritation. Contact with molten material can result in burns.
Carcinogenicity:	N/A

7. EMERGENCY AND FIRST AID PROCEDURES

Inhalation:	Move subject to fresh air.
Eye Contact:	Flush eyes with plenty of water for at least 15 minutes. Call a physician.
Ingestion:	This material is not expected to be absorbed within the gastrointestinal tract, so induction of vomiting should not be necessary.
Skin Contact	If molted material contacts skin, cool rapidly with cold water and obtain medical attention for thermal burn.

HSIN HWA CHEMICAL CO., LTD.

8. REACTIVITY INFORMATION

Stability:	Stable
Conditions to Avoid:	Temperatures over 300° C/570° F
Hazardous Decomposition Products:	Thermal decomposition or combustion may emit vapors, carbon monoxide, or carbon dioxide
Incompatible Compounds:	Acids, bases, and strong oxidizing agents.

9. SPILL OR LEAK INFORMATION

Sweep or scoop up and remove.

10. WASTE DISPOSAL

Landfill or incinerate at a facility that complies with local, state and federal regulations.

11. EXPOSURE CONTROLS/PERSONAL PROTECTION MEASURES

Respiratory Protection:	None required under normal conditions. See Section 12.
Hand Protection:	Canvas or cotton gloves.
Eye Protection:	Safety glasses with side shields (ANSI Z87.1 equivalent).
Other Protection:	N/A
Ventilation:	Local exhaust ventilation systems should be constructed and installed in accordance with ANSI Z9.2 or ACGIH guidelines to control potential emissions near the source.

12. STORAGE AND HANDLING INFORMATION

Maximum Storage Temperature:	99° C/210° F (softening temperature).
Storage Measures:	If material is stored under ambient temperature conditions, it is not hazardous. However, extensive storing at higher than the maximum temperature will emit vapors, carbon monoxide or carbon dioxide.
Handling Measures:	Processing of the material under high temperatures will cause hazardous emissions of vapors, carbon monoxide or carbon dioxide. Blower collecting and local exhaust ventilation systems should be installed to prevent contaminant dispersion into the air. Sawing of

HHC 宏萊實業股份有限公司

HSIN HWA CHEMICAL CO., LTD.

this product generates particulates regulated as "inert" or "nuisance" dusts. To minimize dust emissions, engineering controls should be employed, such as baghouse filters and cyclone separators.

13. REGULATORY INFORMATION

Environment

Comprehensive Environmental Response, Compensation, and Liability Act (CERCLA):	Under section 102(a) of the Act, this product is NOT designated as hazardous. In addition, no reportable quantities and no notification requirements to the National Response Center in Washington, DC are set forth for its release from a vessel, an offshore or an onshore facility (40 CFR Part 302).
Resource Conservation and Recovery Ace (RCRA):	When this product becomes a waste, it is identified as solid but NOT hazardous waste under RCRA criteria (40 CFR Part 261).
Toxic Substances Control Act (TSCA):	The components of this product are on the TSCA inventory list. Any impurities present in this product are exempt from listing.
Superfund Amendment and Reauthorization Act of 1986 (SARA) Title III:	This product may be considered an immediate (acute) health hazard due to potential MMA emissions. However, reporting of thresholds for the material is not required because the concentration of its MMA component is below the de minimis concentration (40 CFR Part 370).

Transportation

DOT Hazard Class:	Not regulated.
DOT Shipping Name:	N/A

Labor Awareness

This product as supplied is non-hazardous under the OSHA Hazard Communication Standard (29 CFR 1910.1200). However, under processing conditions it may become a health hazard to employees because vapors and/or particulates could be released. See Section 12 for Storage and Handling Information.

14. GLOSSARY

ACGIH	American Conference of Governmental Industrial Hygienists
CFR	Code of Federal Regulations
DOT	United States Department of Transportation
mg/m³	milligrams per cubic meter (concentration)
MMA	Methyl methacrylate
MSHA	Mine Safety and Health Administration
N/A	Not Applicable or Not Available
NIOSH	National Institute for Occupational Safety and Health
OSHA	Occupational Safety and Health Administration (Department of Labor)
PEL	Permissible Exposure Limit (time-weighted average)

HHC 宏萊實業股份有限公司
HSIN HWA CHEMICAL CO., LTD.

PMMA	Polymethyl methacrylate
ppm	parts per million (concentration)
STEL	Short-Term Exposure Limit (15-minute)
TLV	Threshold Limit Value (time-weighted average)

The information presented herein is believed to be factual and reliable. It is offered in good faith, but without guarantee, since conditions and methods for the use of our products are beyond our control. We recommend that the prospective user determine the suitability of our products and these suggestions before adopting them on a commercial scale.

الخلاصة

هذا البحث هو دراسه للحفر تحت السطح بواسطة الليزر وقد تحقق باستخدام ليزر نديميوم ياك النبضي وبطولين موجيين 1064 نانومتر و532 نانومترنوعان من الليزرات استخدمت الاول بعرض نبضي 4 نانوثانية و100 مايكرومتر قطر ضوء الليزر والثاني بعرض نبضي 10نانوثانية وقطر اليزر 200 مايكرومترونوعان من المواد الشفافة قد استخدمت في هذا العمل زجاج البوروسليكات والبولي مثيل ميثاكريلات وكل من هذه المادتين كان بسمك 10 ملم

وقد تم دراسة تأثير تغير طاقة الليزر وطول الموجة والموقع البؤري وعدد النبضات ومعدل التغذية ومعدل تكرار النبض لتحديد النقطة المثالية التي ميزت بمجهر الإرسال والمجهر الإلكتروني. وقد تم تحديد شكل النقاط، مساحة السطح و الوضوح مع قياس مساحة السطح وعمق الاختراق. المساحة السطحية للنقاط تزداد بزيادة طاقة الليزر في حين أن وضوح الصورة يمكن السيطرة عليه عن طريق تغيير معدل تغذية CNC ومعدل تكرار النبض. تم الحصول على الظروف المثلى لنقش تحت السطح بواسطة الليزرمع الطول الموجي 532نانومتر، ومعدلات التغذية (2,5ملم/ثا) و(4,3 ملم/ثا) والطاقة 360 مللي جول في 6هيرتز معدل تردد النبض و الطاقة 460 مللي جول في 5هيرتز معدل تردد النبض وكانت النتائج الأقل التي تم الحصول عليها في معدل التغذية (1,56 ملم/ثا) و (8,5ملم/ثا) و الطاقة 360 مللي جول مدة نبض 6هيرتز .تم محاكاة الحفر بالليزر تحت السطح باستخدام برنامج COMSOL Multiphysics. نموذج انتقال الحرارة يوفر توزيع درجة الحرارة داخل المواد والنقاط أبعاد تم قياسها و قورنت مع النتائج التجريبية، وكانت قريبة جدا من بعضها البعض في القيمة ومتشابهة في الشكل.

الاهداء

الى منبع الحب والعطاء

عائلتي

امي , ابي

اخي واخواتي

والى

زوجي الحبيب

دمت لي سندا وامانا

الحفر تحت السطح للبوروسليكات والبولي مثيل ميثاكريلات باستخدام ليزر نديميوم ياك ذي مفتاح عامل النوعية

رسالة مقدمة الى

معهد الليزر للدراسات العليا /جامعة بغداد /لاستكمال متطلبات نيل شهادة ماجستير علوم في الليزر/ الهندسة الميكانيكية

من قبل

زهراء محمد صالح

بكالوريوس هندسة ميكانيكية 2006

بإشراف

الدكتور زياد اياد طه

1438 هـ   **2017 م**